The Effect of Using Transverse Partitioning and Reflection on Single and Counter Flow Solar Air Heater Using Wire Mesh as an Absorber

Monther Fuad Al-Khawajah

Submitted to the
Institute of Graduate Studies and Research
in partial fulfillment of the requirements for the Degree of

Doctor of Philosophy
in
Mechanical Engineering

Eastern Mediterranean University
September 2011
Gazimağusa, North Cyprus

Approval of the Institute of Graduate Studies and Research

_____

Prof. Dr. Elvan Yılmaz
Director

I certify that this thesis satisfies the requirements as a thesis for the degree of Doctor of Philosophy in Mechanical Engineering.

_____

Assoc.Prof.Dr. Ugur Atikol
Chair, Department of Mechanical Engineering

We certify that we have read this thesis and that in our opinion it is fully adequate in scope and quality as a thesis for the degree of PHD in Mechanical Engineering.

_____

Assoc. Prof. Dr. Fuat Egelioğlu
Supervisor

Examining Committee

1. Prof. Dr. Hikmet Aybar _____
2. Prof. Dr.Kahraman Albayrak _____
3. Assoc. Prof. Dr. Fuat Egelioğlu _____

ABSTRACT

Rising costs of conventional fuels, increasing energy demand, concerns over climate change and pollutants resulted from burning fossil fuels have increased the interest in various renewable energy technologies. The energy demand associated with heated air for different sectors is quite significant. Solar air heaters have been developed with the aim of reducing the demand for conventional fuels. 3 glazed solar air heaters were experimentally studied here.

The thermal performance of a single and counter path solar air heater with 2, 4, and 6 fins attached were experimentally investigated. The effect of reflection on the single path solar air heater with 2 fins was studied. Wire mesh layers were used between the fins instead of an absorber plate. The effects of mass flow rate of air on the outlet temperature and thermal efficiency were studied. The indicated results show that the efficiency always increases with increasing the mass flow rate for the range of the flow rate used in this work. The maximum efficiencies obtained for the counter pass solar air heater (CPSAH), and the single pass solar air heater (SPSAH) for the 6 fins case and mass flow rate of 0.042 kg/s were 85.9% and, 79.8% respectively. While the maximum efficiency obtained for single pass solar air heater with reflection (SPSAHWR) was 56.1% compared to 65.8% for the 2 fins SPSAH case and same mass flow rate.

In addition, the maximum instantaneous temperature difference obtained for CPSAH, and SPSAH, was 62.1 ^{o}C, 51 ^{o}C, respectively for the 6 fins SAH when the mass flow rate was 0.0121 kg/s. While the maximum instantaneous temperature difference obtained for SPSAHWR was 51.1 ^{o}C compared to 44.2 ^{o}C of SPSAH of the same mass flow rate.

Comparison of the results of CPSAH, SPSAH and SPSAHWR collectors with those of a conventional collector shows a substantial enhancement in the thermal efficiency.

Keywords: Renewable energy, solar air heaters, counter path solar air heater with fins, single path solar air heater with fins, thermal efficiency.

ÖZ

.

Artan konvansiyonel yakıt maliyetleri, artan enerji talebi, iklim değişikliği endişesi, ve fosil yakıtların yanmasından çıkan kirlilik, yenilenebilir enerji teknolojilerine olan ilgiyi artırdı. Farklı sektörlerin ısıtılmış havaya olan talebi oldukça önemlidir. Konvansiyonel yakıt tüketimini azaltmak için güneş hava ısıtıcıları geliştirildi. Bu çalışmada 3 camlı güneş ısıtıcısı deneysel olarak çalışıldı.

Tek ve çift geçişli, 2, 4, 6 kanatçıklı güneş hava ısıtıcılarının termal performansı deneysel olarak araştırıldı. Güneş yansımasının tek geçişli 2 kanatçıklı güneş hava ısıtıcısına etkisi araştırıldı. Emici metal plaka yerine kanatçıkların arasında tel örgü tabakaları kullanıldı. Hava kütlesi akış hızının termal verimliliğe ve havanın çıkış sıcaklığına olan etkileri araştırıldı. Elde edilen neticelerde bu çalışmada kullanılan hava kütlesi akış hızının artmasıyle verimliliğin sürekli arttığı görülmüştür. Çift geçişli güneş hava ısıtıcısında ve tek geçişli güneş hava ısıtıcısında elde edilen en yüksek verimlilik 6 kanatçık ve 0.042 kg/s hava akış hızında sırasıyla %85.9 ve %79.81 idi. İki kanatçıklı tek geçişli yansıtıcılı güneş hava ısıtıcısında elde edilen en yüksek verimlilik %56.1'e kıyasla, aynı hava akış hızında iki kanatçıklı tek geçişli güneş hava ısıtıcısında elde edilen en yüksek verimlilik %65.8 idi. Altı kanatçıklı çift geçişli güneş hava ısıtıcısında ve tek geçişli güneş hava ısıtıcısında elde edilen en yüksek ani sıcaklık değişimi 0.0121 kg/s akış hızında sırasıyla 62.1 ^{o}C ve 51 ^{o}C idi. Ayrıca, iki kanatçıklı tek geçişli yansıtıcılı güneş hava ısıtıcısında ve tek geçişli güneş hava ısıtıcısında elde edilen en yüksek ani sıcaklık değişimi 51.1 ^{o}C ve 44.2 ^{o}C idi.

Çalışılan sistemlerde elde edilen neticeler ışığında bu ısıtıcılar konvansiyonel güneş ısıtıcılarına kıyasla oldukça yüksek verimliliğe sahiptirler.

Anahtar Kelimeler: Yenilenebilir enerji, güneş hava ısıtıcısı, kanatçıklı çift geçişli güneş hava ısıtıcısı, kanatçıklı tek geçişli güneş hava ısıtıcısı, termal verimlilik.

ACKNOWLEDGMENT

I seize this opportunity to express my sincere gratitude to my thesis supervisor Assoc. Prof. Dr. Fuat Egelioğlu. And to acknowledge the help I received from Assoc. Prof. Dr. Loay B.Y Aldabbagh. Furthermore, I am extremely grateful to all my instructors and the entire staff of the Mechanical Engineering Department for giving me the opportunity to carry out my graduate studies and this research.

In particular, I am thanking my wife, my sons and my daughters for their emotional support and encouragement, as through them, I found the motivation and focus to complete this project.

TABLE OF CONTENTS

LIST OF TABLES

LIST OF FIGURES

LIST OF SYMBOLS/ABBREVIATIONS

SAH……Solar air heater

SWH……Solar water heater

SPSAH……Single path flow solar air heater

CPSAH……Counter path flow solar air heater

SPSAHWR……Single path solar air heater with reflection

MA……Mean average value

A_c …… Area of the collector (m^2)

C_p …… Specific heat of air (kJ/kg. K)

I …… Solar radiation (w/m^2)

m…… Air mass flow rate (kg/s)

T_{out} …… Outlet temperature (K)

T_{in} …… Inlet temperature (K)

T_f……..the film air temperature between the outlet and inlet(T_{out} + T_{in})/2

ΔT …… Temperature difference (T_{out} - T_{in}) (K)

ΔT_b……Bed temperature difference (T_b- T_{in}) (K)

ΔT_g……Glass temperature difference (T_g - T_{in}) (K)

η …… Efficiency of the solar collector $\eta = \frac{m C_p (T_{out} - T_{in})}{I A_c}$

Q……..Volume flow rate (m^3/s).

A_2 …… Area of small diameter for orifice $\frac{\pi}{4} d^2$ (m^2).

CM …… Flow coefficient, 0.64

ρ ……..Density of air (kg/m^3).

ΔP…… Pressure difference, (N/m^2).

ρ_a …… Density of alcohol, 803 (kg/s).

g ……Gravitational acceleration(m/s^2)

h ……level change inside the incline manometer (m)

ω ……..……..……The uncertainty

Chapter 1

INTRODUCTION

1.1 Solar Energy and Its Availability

Solar energy could directly provide all the necessary energy requirements for human need. If it could be collected from only 1% of the earth's surface, the human population's power supply could be entirely supplied directly by the sun (Kalogirou, 2009).

Solar radiation available to the earth's surface is also much less than the radiation available outside the earth's atmosphere. Approximately 25-50% of the solar radiation outside the earth's outer atmosphere is lost upon entering it. The greenhouse gases and water vapor reflect and absorb much of the energy radiated to the earth. (Goswami et al. 2000)

1.2 Solar Energy Utilization

The emergence of interest in solar energy utilization has taken place since 1970, principally, due to the rising cost of energy from conventional sources. Solar radiation is the world's most abundant and permanent energy source. There are many areas where the solar energy is obviously used such as:

- Industrial process heating
- Electricity generation (Solar thermal power plant, photovoltaic systems)
- Greenhouse heating
- Swimming pool heating

- Domestic hot water heating : Evacuated-tube solar collectors, integral collector- storage systems, flat-plate collector
- Space heating and cooling

1.3 Types of Solar Heaters

Solar heater is simply a system that absorbs solar energy by using its available surface area to capture the sun's radiation. Different methods are used in classifying solar heaters. One of these classifications, is based on the working fluid as an example of water solar collectors and air collectors or alcohol solar collectors. Another classification depends on the application of the solar collector such as domestic use and industrial use. In literature, some classifications can be found based on their mechanism and design such as fixed and movable solar collectors or single path and double path or single glazing and double glazing. Others divided the collectors based on the absorber plate and solar traction system such as concentrated or flat collectors.

As a result of this, there is no rigid classification that can be used in our research. However, as it will be seen soon in this thesis, the classifications that are used are either the design of the absorber plate or the flow direction of used air.

1.4 Solar Air Heater (SAH)

Conventional solar air heaters mainly consist of panels, insulated hot air duct and air blowers in active systems, without having blower in the passive system. The panel consists of an absorber plate and one or two transparent covers to allow solar radiation to penetrate into the collector. The plate of SAH (usually painted with the black color to maximize absorption) absorbs the solar radiation, and then transfers

the heat to a fluid. The working fluid flows through the SAH over the plate, thereby collecting the heat absorbed by the plate via convection.

SAHs are cheap and extensively used. It has wide range of application such as delivering heated air at low to moderate temperatures for space heating, drying agricultural products (i.e., fruits, seeds and vegetables), and in some industrial applications (Akpinar et al., 2004).

SAHs are environmentally friendly, i.e., pollution free, sustainable, financially competitive, and safe (flammability and explosively). The SAHs have different advantages compared to water solar collectors such as SAHs are free of freezing, corrosion, or leakage problems.

Typical flat plate collectors can obtain outlet fluid temperatures of around 70 °C. The thermal efficiency of these collectors depends on the working fluid, but simple flat plate solar heaters can have efficiencies of about 60% for solar water heaters (SWHs), and about 40% for SAHs for normal operating conditions (Goswami et al. 2000).

1.5 Literature Review

Different factors affect the SAH effectiveness such as collector dimensions, type and shape of absorber plate, glass cover, inlet temperature, wind speed and etc. (Aboul-Enein,S. 2000). However, the most important mentioned factors are the glass cover and absorber plate. The coming sections will briefly discuss the previous work of researchers in improving the effect of these factors.

1.5.1 Absorber Plate

As it is mentioned before, the absorber plate is one of the important parameters that affect the SAH performance. As a result of this, several configurations of

absorber plates have been designed by different researchers to improve the heat transfer coefficient. Artificial roughness, obstacles and baffles in different shapes and arrangements were employed to increase the area of the absorber plate. As a result of this, the heat transfer coefficient between the absorber plate and the air path will be improved (Romdhane, ben salma, 2007, Varun, Amar et al, 2008,Varun, Amar et al, 2009, Garg, and Adhikari R.S. 1999, Alvarez, A.et al., 2010, Gupta, M.K. and Kaushik, S.C., 2009).

Literature review shows that (Suleyman Karsli,2007) the efficiency of the solar air collectors depends significantly on the solar radiation and surface geometry of the collectors.

Esen, H. (2008) investigated experimentally, for mass flow rate between 0.015 kg/s and 0.025kg/s, the introduction of the obstacles fixed on the absorber plate. He could improve the efficiency up to 45% by his proposed design. Youcef-Ali (2005), Youcef-Ali et al. (2006, 2007) indicated that the maximum thermal efficiency which could be obtained, equals to 68% with pressure drop more than 50 Pa at mass flow rate less than 0.0152 kg/s for the offset rectangular plate fins design. Ozgen, F. et al (2009) investigated experimentally the effect on efficiency by inserting an absorbing plate which made of aluminum cans into the double-path channel in a flat-plate SAH. They argued that this configuration substantially improved the collector average efficiency up to 0.55 at mass flow rate 0.05 kg/s. An energy analysis and flow characteristics of finned SAH was analyzed experimentally and numerically by Alok et al.(2006), Moummi et al. (2004), and Flores-Irigollen et al. (2004).

As a summary, fins and obstacles have been proposed as an effective way of improving the heat transfer from the SAH absorber plates. On the other hand, fins

pose difficulty in manufacturing the plates and significant increase in the cost. As a result, this SAH still identifies room for greater improvement in efficiency.

Including the use of packing of porous materials like wire screens (Mittal, and Varsheny, 2006), cross rod matrices aluminum-foil matrices, steel wool (Sopian, 2007) and etc., in the duct of a SAH have been proposed for the enhancement of thermal performance. Porous media increases the turbulence and mixing of the flowing air so the heat transfer coefficient between packing elements and air increases. Another advantage of using porous medium is that it tends to increase the surface per unit volume ratio (Mittal and Varshney 2006). Much of research has concentrated on experimental work, although some researchers developed some models, due to the complex nature of heat transfer through porous media. On the other hand, the disadvantage of using the porous media is that the porous media increases the pressure drop across the channel. Kolb et al. (1999) suggested a new bed design using two layers of wire mesh fixed on the absorber plate in order to overcome the increases of pressure drop across the channel of the SAHs. They analytically investigated their suggestion and reported that the thermal efficiencies were between 58% and 81% for the range of air mass flow rates between 0.0100 kg/s and 0.0367 kg/s. The maximum pressure drop mentioned in their work was 19 Pa. A.A.Mohamad (1997), basing on his numerical solution, reported that the pressure drop is a function of porosity where it cannot be high for the porosity more than 0.85. El-Sebaii et al. (2007) used two different configurations, limestone and gravel as a packed bed materials, and obtained experimentally a thermal efficiency up to 65% at 0.05kg/s mass flow rate, where the pressure drop was 400 Pa. He recommended to operate the system with a packed bed with less than 0.05kg/s in order to have a lower pressure drop across the system, and therefore, a reasonably high thermal efficiency. The effect of porosity on the

transferred heat was studied experimentally by Thakur et al. (2003). This investigation covers a wide range of geometrical parameters of wire screen matrix, i.e. wire diameter 0.795 to 1.4 mm, pitch 2.5 to 3.19 mm and number of layers from 5 to 12. They reported the decrease in porosity increases the volumetric heat transfer coefficient.

Parasad et al. (2009) presented an experimental investigation which had been carried out on a packed bed SAH using wire mesh as a packing material for air flow rates ranging from 0.0159 to 0.0347 kg/s. They reported that the efficiency of the packed bed SAH with porosity of 0.599 increased from 53.3% to 68.5% compared to the conventional SAH. Moreover, they mentioned that the efficiency increased by decreasing the porosity of the bed. Paisarn (2005) numerically studied the heat transfer characteristics and the performance of the double-path flat plate solar air heater with and without porous media. He reported that the efficiency was varied from 38% up to 59% for the bed without porous media, and it was varied from 42% to 70% with porous media for mass flow rates between 0.03 and 0.07 kg/s respectively. Recently there is a considerable work which used wire mesh instead of the absorber plates. Aldabbagh et. al (2010) proposed a new SAH with 10 wire mesh layers as an absorber plate. Omojaro and Aldabbagh (2010) used longitudinal fins with 7 wire mesh layers in between for single and double path SAH.

1.5.2 Cover Heat Losses

Major heat losses from flat- plate solar collectors are found to be through the top cover; heat losses from the bottom and the sides of the collector are low as they are adequately insulated. In order to minimize the heat losses and improve the efficiency, double glazing was recommended by several researchers, Martin, SRL.and Fjeld, GJ. (1975), Prasad et al. (2009). The best results were obtained by Parasad et al. (2009) who reported that the maximum efficiency which could be obtained by this

improvement and using the porous media was 68.5% for the design and working parameters that mentioned in the previous section.

Some others suggested to insert the absorber plate into the middle of the SAH channel, so that the air will pass above the absorber plate then directed to pass below it (Sopian et al., 1999; Sopian et al. 2009) or vice versa (Ho et al., 2005, Lertsatitthanakorn et al., 2008) or to flow above and below the absorber at the same time (Yeh et al., 2002; Ozgen et al 2009). The best obtained efficiency (60%-70%) was by Sopian when he used double path collector with porous media in the second channel.

Some other researchers introduced a counter flow or what is called an external recycle by some of the other researchers, where the air is forced to flow over the lower glass before passing through the absorber (Mohamad, A.A.,1997, Yeh and Ho, 2009 [a], Yeh, and Ho, 2009[b], Hoa et al., 2005). The application of external-recycle operation to SAHs actually has two conflict effects. The first effect is the desirable effect of increasing fluid velocity to decrease the heat transfer resistance, and the second is the undesirable effect of decreasing the driving force (temperature difference) of heat transfer, due to the remixing at the inlet. It is found that considerable improvement in collector efficiency is obtainable if the operation is carried out with an external recycle, where the desirable effect overcomes the undesirable effect.

1.6 Reflection in SAH

In solar energy applications that require high temperatures, such as thermal power generations, solar energy can be optically concentrated before being transferred into heat, thereby increasing the thermal effect of the device. The reflected radiation is

concentrated in a local zone, thus increasing the energy flux in the receiving target. (Hsieh, 1986)

Two types of reflecting surfaces can be used: concave or flat surfaces. The concave ones are more complex in nature as it becomes essential to maintain a normal angle to the sun. Such collectors result in much higher capital costs and, therefore, the more common method for collecting solar thermal energy is a flat surface reflector.

Many theoretical and experimental studies have been done to investigate the effect of reflections on SAHs. The parametric study has been made by Tyagi et al. (2007) for different mass flow rates and concentration ratios using hourly solar radiation. Most of the performance parameters, such as, output energy, the inlet temperature, ambient temperature etc. increase as the solar intensity increases. The performance parameters, mentioned above, are found to be the increasing functions of the concentration ratio

An indirect forced convection with desiccant integrated solar dryer has been built and tested by Shanmugam and Natarajan (2007). The effect of reflective mirror on the drying potential of desiccant unit was also investigated. With the inclusion of a reflective mirror, the drying potential of the desiccant material is increased by 20% and the drying time is reduced. The temperature rise was about 10 ^{o}C by using the mirror.

In reflection, more extra operational and design parameters affected the SAH more than what is mentioned at the beginning of the literature review. These parameters include collector-reflector system orientation and tilt angles, collector elongation ratio, and reflector overhang ratio. The effects of such parameters were studied by Hussein et al. (2000). The case of study was at latitude 30^{o}N and the

length of the reflector equals to the length of the bed. They concluded that the optimum tilt angle is the angle, at noon time, which covers the longest distance of the bed. In addition, they reported that the south facing reflector provides higher yearly solar energy collection than the north facing one.

However, Tanaka (2009, 2011) theoretically predicted the distillate productivity of a tilted-wick solar still with an inclined flat plate external reflector extending from the back wall of the still on a winter solstice day at 30^{o}N latitude, and the results of this work were summarized as follows:

(1) The solar radiation absorbed on the absorbing plate of the collector can be increased by using a flat plate top reflector, which is inclined forwards in winter and backwards in summer, and by setting the inclination angle of the reflector at less than 30^{o} throughout the year. When the reflector's length is a half of or the same as the still's length,.

(2) The optimum reflector inclination is considerably affected by the ratio length of reflector compared to the length of the bed, and will increase with an increase in the ratio.

1.7 Objectives and Thesis Organization

It is seen that in the literature review there is a shortage in experimental work involving the use of fins with porous media working as an absorber plate in a counter flow SAH or reflection.

The main objectives of the present project are to perform outdoor experiments on a proposed advanced unique SAH. The output parameters and capabilities of the collector will be explored and documented, with the intent of determining usefulness.

The specific objectives can be summarized in the following points:

- To construct the mentioned advanced solar air heating collectors.
- To perform outdoor testing over an extended period of time.
- To perform an analysis of the data collected by continuous operation of the collector.
- To assess the performance of the collector with different cases and feasibility of the collector for the Cyprus environment.

In order to provide an understanding of the work already contributed to solar air heating, and further understand the modifications and contributions the present collector makes to solar air heating, a discussion of solar air heating technology will be presented in the following chapters.

In chapter 2, the experiment is defined and the experimental set up is described. Chapter 3 investigates the first part of the study: SPSAH having transveres fins attached and steel wire mesh as porous media. In chapter 4, The effect of using transverse fins on a CPSAH using wire mesh as an absorber is presented. Also in this chapter a comparison of the SPSAH results of chapter 3 and the double pass of chapter 4 will be compared and discussed. Chapter 5 deals with the reflection part and comparing the reflection results with the results obtained in other chapters. Chapter 6 presents the general conclusions and recommendations. Future works are also presented in this chapter.

Chapter 2

EXPERIMENTAL PROCEDURE

As discussed in the previous chapter, conventional SAH mainly consists of panels, insulated hot air ducts and air blowers in active systems, forming a passage for airflow. A glass or plastic cover is fixed above the absorber plate and the system is thermally insulated from the back and on the sides.

The following sections will discuss the new designed SAHs used in the experiments, the measurements devices, calibration process, and the experimental procedure.

2.1 Apparatus

Three different set ups were designed and constructed in order to obtain data for the investigation. The schematic of the SPSAH and the CPSAH types are shown in fig. 2.1 and fig. 2.2 respectively. Fig 2.3 and fig 2.4 show the pictorial view of the experimental set up for the SPSAH and the SPSAHWR. The first and second types consist of three different designs based on the number of fins in the bed. The effect of reflection on the performance of SAH is studied on one designed case.

2.1.1 The Bed

In the three different types of collectors the bed consists of a wooden box, 150 cm long and 100 cm wide. The frame of the collector was made of 2 cm thick plywood

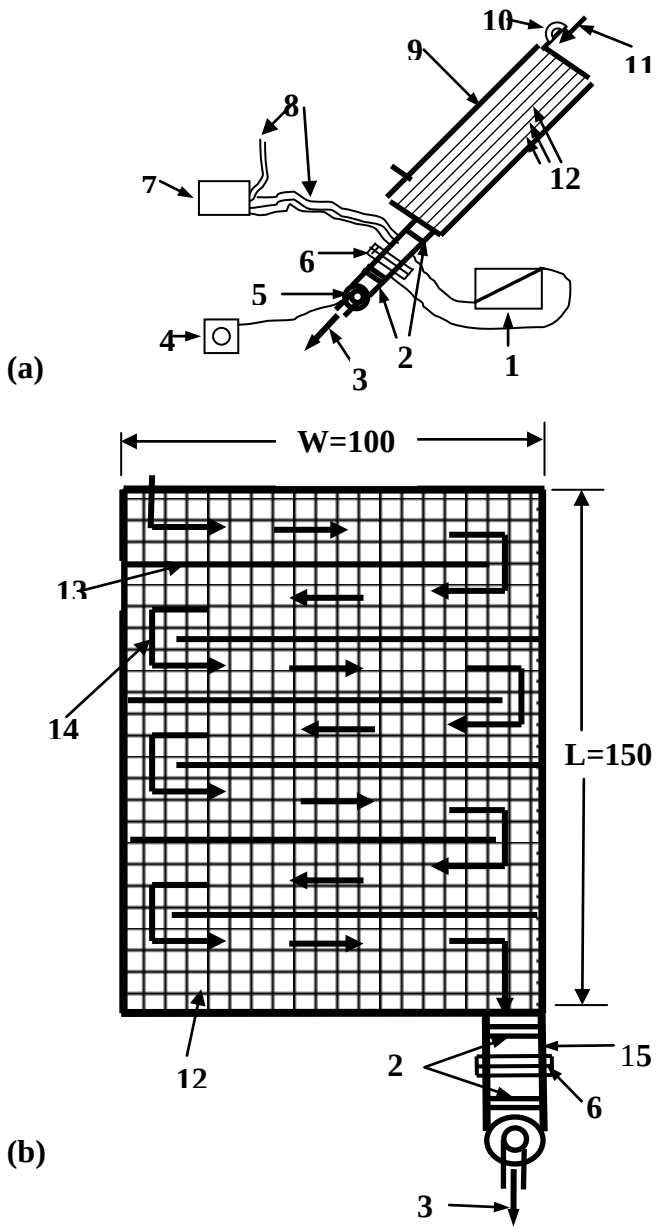

1-Incline manometer 2- Straightener
3- Discharged air 4- Speed controller
5- Fan 6- Orifice meter
7- Digital thermometer 8- Thermocouples
9- Glass 10- Pyranometer
11- Inlet flow 12- Wire mesh
13- 6 transverse fins (Barriers) 14- Air flow direction
15- Steel pipe

Figure 2.1: SPSAH (a) Schematic assembly of the SPSAH system (b) front view of Collector

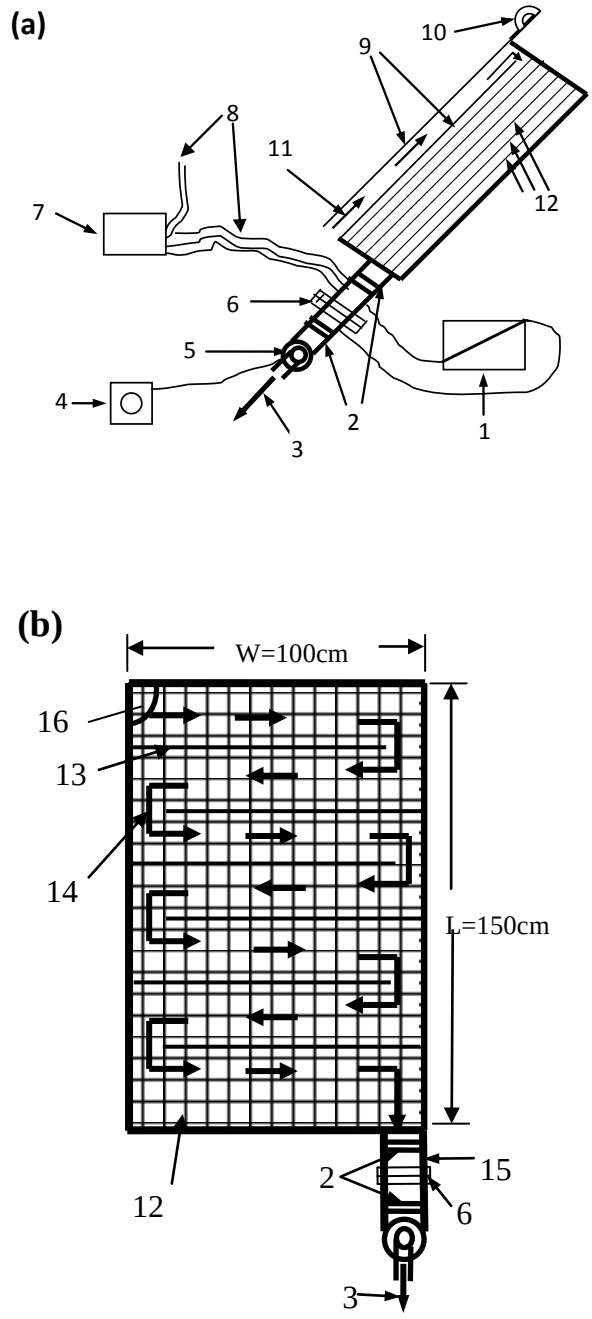

1-Incline manometer	2- Straightener
3- Discharged air	4- Speed controller
5- Fan	6- Orifice meter
7- Digital thermometer	8- Thermocouples
9- Glass	10- Pyranometer
11- flow of air between glasses	12- Wire mesh
13- 6 transverse fins (Barriers)	14- Air flow direction
15- Steel pipe	16- inlet air gap into the matrices

Figure 2.2: CPSAH (a) Schematic assembly of the CPSAH system (b)Front view of collector

Figure 2.3: Pictorial view of the experimental set up for SPSAHWR .

Figure. 2.4 Pictorial view of the experimental set up for SPSAHWR .

internally painted with black and externally insulated with 2cm thick Styrofoam. A window glass of 0.4 cm thicknesses was used as glazing for the SPSAH and the SPSAHWR, while two similar glasses were used for CPSAH type. The distance between the upper glass and the lower glass is fixed to be 3 cm and a quarter circle orifice is done in the top left corner of the lower glass for air inlet in the case of CPSAH, see fig. 2.2 (b).

The distance between the second glass and the bottom of the collector in the CPSAH was fixed to be 7 cm. In order to find the effect of the fins on the efficiency and the outlet temperature 2, 4, and 6 steel fins were installed in the collector and investigated separately for both cases of SPSAH an CPSAH, while just 2 fins for the SPSAHWR. The length, height and thickness of each fin were 50 cm, 7 cm and 0.1 cm respectively (Fig. 2.1 (b) and Fig. 2.2 (b)). The fins were painted with black color and positioned transversely along the bed such that three, five and seven equally spaced sections were created. A flexible black slot rubber of 0.4 cm thickness and 0.4 cm depth was fixed between the glass and each of the fins. In this way, air flows in a snake path picking up heat as it goes along the passage channel. As the path length was increased by increasing the number of fins, the velocity of air was also increased for the same air mass flow rate as the cross-sectional area of the air passage channel decreased.

2.1.2 Porous Material

The porous material was placed in the bed using small wooden frame 0.5*0.5 cm cross section to hold it, thereby heat losses are reduced and the layers in matrices are organized. Each matrix in the bed was packed using six parallel layers, positioned parallel to the glazing, with 1cm distance between one and the other to reduce the pressure drop through the channel. The layers consist of different numbers of

parallel steel wire mesh sheets of 0.18 cm × 0.18 cm in cross sectional opening, and a 0.02 cm diameter wire were used. The number of sheets in the layers was based on an experimental work in measuring the penetrated distance of solar radiation through the layers of the wire mesh (porous media). The total number of sheets were 12, arranged in 6 layers with 3,3,2,2,1,1 sheets from bottom to top respectively.

The matrices were painted with black color before installing them between the fins (Fig.2.1 & Fig.2.2). These matrices replaced the absorber plate in the traditional SAH, Hence, this design is cheaper if compared to the SAHs having absorber plates. The porosity of the bed was calculated as the (total volume occupied by solid- the solid volume) divided by the total volume and a value of 0.966 was obtained.

The volume ratio was obtained by using the wetting liquid method. A known dimension piece of the wire screen is immersed in a container filled with water; the displaced water is equal to the volume of the solid. Subtracting the displaced water from the total volume of the specimen gives the void per unit area of the wire mesh. Since the total used area of wire mesh is known, then the total volume of solid can be found. Dividing the volume of the solid on the volume of the bed the porosity is obtained. However, the obtained result was so close with the calculated one.

With this modification, the cost of the SAH is reduced considerably because the wire mesh is readily available in the market and very cheap. In addition, the new design of the porous matrices will reduce the pressure drop due to the porous medium used in the SAH. At higher porosity, there is always a reduction in pressure drop and storage heat in the bed.

2.1.3 Connecting Ducts

Two connecting ducts were used in the experimental set up. One was used to connect the exit of the collector to the inlet of the orifice (30 cm long). It starts with

a converging section to change the exit orifice from rectangular shape (20cm x 5cm) to circular duct (11 cm in diameter). It is thermally insulated by 2 cm Styrofoam to reduce heat losses to the surroundings. Another aim of using this duct is to mix the exit heated air as this reduces the needed number of readings to find the exit bulk air temperature.

The second connecting pipe with 11 cm in diameter was fixed between the exit of the orifice meter and the fan. It is 30 cm long and not insulated.

2.2 Measurements and Calibration of the Instruments

2.2.1 Air Flow

A calibrated orifice meter is installed on the discharge pipe of 11 cm diameter and 60 cm length for measuring the volume of flow rate of the air. The orifice meter was designed according to Holman (1989) as shown in fig. 2.4. It is installed in the pipe before the blower fan.

The flow rate can be found by the following equation:

$$Q = CM\ A_2 \sqrt{\frac{2\ g_c}{\rho}} \sqrt{\Delta P} \qquad (2.1)$$

Where:

Q volume of flow rate, (m^3/s).

A_2 area of small diameter, (m^2).

CM flow coefficient, 0.64

ρ density of air, (kg/m^3).

g_c specific gravitational force, ($1kg.m/N.s^2$)

ΔP pressure difference, $P_2 - P_1$, (N/m^2).

Substituting the numerical values into equation 2.1 and after calibration, yields to

$$Q = 0.002148\sqrt{\Delta P} \qquad (2.2)$$

In order to get a uniform flow through the orifice meter, two flow straighteners were installed inside the pipe before and after the orifice. Each straightener consisted of plastic straw tubes with 0.4 cm diameter and 5 cm long.

A calibrated inclined manometer was used to measure the pressure drop through the orifice meter. It was tilted to 15.5^{o} to have more accurate results. In addition, alcohol with a density of $803 kg/m^3$ was used as a fluid inside the manometer to increase the accuracy of the measured pressure through the orifice meter.

2.2.2 Temperature Measurements

Thermocouples (T-type) were placed at different locations and compartments of the collector and corresponding inner and outer glass, so that the amount of useful energy from the collector will be determined and the thermal performance comparison between the different models and cases can be made.

The outlet, T_{out}, and the inlet, T_{in}, temperature were measured by using four T-type thermocouples. Two thermocouples were fixed inside the pipe before the orifice meter to measure the outlet temperature of the working fluid from the collector, while two thermocouples were fixed underneath the solar collector to measure the ambient air temperature (T_{in}). In this case the ambient temperature and the temperature of the inlet are same.

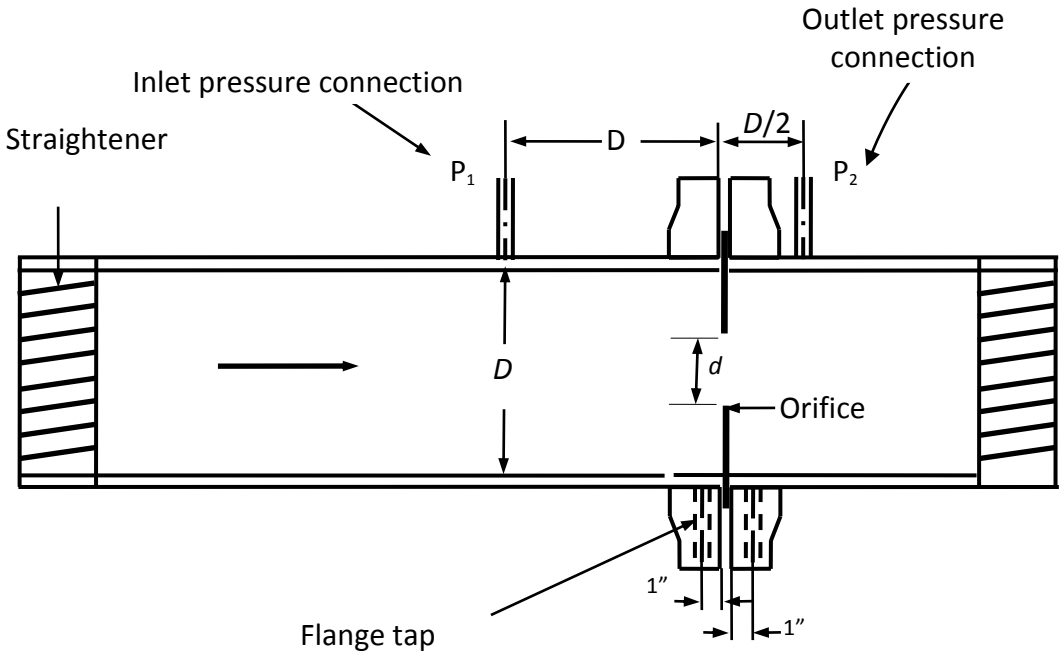

Figure 2.5: Cross sectional view of the designed orifice meter

The glass temperature was measured by using 6 thermocouples which are equally spaced throughout the length of the inner and upper glass on the internal face of the two glasses in CPSAH or 3 thermocouples for the SPSAH. The temperature readings were collected by Ten-channel Digital Thermometer (MDSSi8 Series digital, Omega) (fig. 2.6 a) ±0.5 ^{o}C accuracy. A calibration test showed that the accuracy of the thermocouple readings were within ±0.15 ^{o}C. However, in some cases, an extra digital of Xplorer GLX Pasco data logger of model PS-2002 is used to measure the temperature for the inlet and outlet in the case of SPSAHWR.

2.2.3 Solar Flux

The global solar radiation incident on an inclined surface was measured by using an Eppley Radiometer Pyranometer (PSP) (fig. 2.6 b) coupled to an instantaneous solar radiation meter model HHM1A digital, Omega 0.25% basic dc accuracy and a resolution of ±0.5% from 0 to 2800 W/m^2. The pyranometer was fixed beside the glass cover of the collector.

a)

b)

Figure 2.6: Equipments used in the experiment a) Ten channel thermometer. b) An Eppley Pyranometer.

2.3 Experimental Procedure

The experimental work was performed at the outdoor of the roof of the Mechanical Engineering Department, Eastern Mediterranean University under Famagusta prevailing weather conditions during the summer months, 21.05.2010-20.07.2010, while the reflection part was done during the period of 15-05-2011 to 30-05-2011, with a clear sky condition. Famagusta is a city in Cyprus located on 35.125^{o} N and 33.95^{o} E longitude. The roof was flat, hence, the collector was proposed to be tilted with 35^{o}

Generally, the sky in Famagusta was clear all through the month of May to August with cloudy or partially cloudy from time to time. To observe an accurate reflection of the SAH performance, the data which was collected during more consistent weather condition was studied and considered. However some days were ignored in the analysis because of the weather conditions. The instantaneous values which were taken from the metrological office of Famagusta city was hourly recorded i.e. average mean value of the wind speed and relative humidity ratio.

The experiment has been performed in three main Parts (SPSAH, CPSAH, and CPSAHWR). The first and second parts consist of three different cases (2, 4, 6 fins) and each case has been studied at 6 different mass flow rates (0.0121 kg/s, 0.0171 kg/s, 0.0243 kg/s, 0.0301 kg/s, 0.0364 kg/s, and 0.0420 kg/s), while the last part consists of one case which is at 2 fins at the same of the previous mentioned 6 different mass flow rates.

Although the air was circulating continuously, the inclined tube manometer reading was hourly adjusted 15 min prior to the time in which data were taken.

The measured variables were: T_{in}, T_{out} , wind speed, relative humidity ratio, solar intensity radiation, and the temperature of three different equal places along the

inner face of the glass for SPSAH or the inner faces of both, the lower and upper glass for the CPSAH case were hourly recorded. On the other hand, the pressure drop across the bed was recorded once a day. Finally, the bed temperature at three different equal spaces along the bed of SPSAH and CPSAH was recorded for all the days of 4 fins SAH collecting data. All tests began at 8 am and ended at 5 pm. The experiment was run up to 10 pm for two days to study and estimate the amount of heat stored in the bed of the SAH.

2.4 Uncertainty Analysis

Errors associated with the experimental measurements are presented in the previous section. In this section the uncertainties due to the air mass flow rate and the thermal efficiency are presented.

The equation for mass flow rate across the bed is:

$$m = \rho Q \tag{2.3}$$

Where, ρ (air density) depends on the air temperature and Q (volume flow rate) depends on the pressure difference at the orifice and temperature.

The fractional uncertainty, ω_m / m, for the mass flow rate (Holman,1989, Esen, 2008) is:

$$\frac{\omega_m}{m} = \left[\left(\frac{\omega_{T_f}}{T_f} \right)^2 + \left(\frac{\omega_P}{P} \right)^2 \right]^{1/2} \tag{2.4}$$

The efficiency of the solar collector, η, is defined as the ratio of energy gain to solar radiation incident on the collector plate,

$$\eta = \frac{m C_p (T_{out} - T_{in})}{I\ A_c} \tag{2.5}$$

Since A_c is constant and assuming C_p as constants for the range of working temperature, the fractional uncertainty for the efficiency is a function of ΔT , m, and I. It and can be given as:

$$\frac{\omega_\eta}{\eta} = \left[\left(\frac{\omega_m}{m} \right)^2 + \left(\frac{\omega_{\Delta T}}{\Delta T} \right)^2 + \left(\frac{\omega_I}{I} \right)^2 \right]^{1/2} \qquad (2.6)$$

Performance investigations for different numbers of fins and mass flow rates were carried out; the average values of each variable were daily calculated. Then, the mean of the average values of each variable for all the days of the SPSAH, CPSAH and SPSAHWR were obtained and used to calculate the fractional uncertainty. Table (2.1) shows the calculated mean average values for the variables in the experiment.

Table 2.1: Error analysis of the experimental data

case \ Variable	*MA* ΔT (^{o}C)	*MA* T_{in} (^{o}C)	*MA* T_{out} (^{o}C)	*MA* T_{air} (^{o}C)	*MA* m (kg/s)	*MA* I W/m^2	*MA* η (%)	fractional uncertainty of m ω_m	fractional uncertainty of η ω_η
SPSAH	25.8	27.2	53.0	40.1	0.027	754.35	55.9	0.011	0.022
CPSAH	28.5	32.9	57.7	44.4	0.27	662.95	67	0.0081	0.01
CPSAHWR	26.9	29.19	56.25	42.7	0.02085	833.5	42.8	0.014	0.023

Chapter 3

SINGLE PATH FLOW SOLAR AIR HEATER

This chapter presents the first session of this experimental study. It covers the investigation of the SPSAH. The experiment was carried out between 21.05.2010–20.07.2010, during the summer months under Famagusta (35.125^{o} N and 33.95^{o} E longitude). The experiment was performed for six different mass flow rates of 0.0121kg/s, 0.0171kg/s, 0.0243kg/s, 0.0301kg/s. 0.0364kg/s and 0.0342kg/s. The experiments were carried out from 8.00hrs to 17.00hrs at time intervals of one hour each day.

3.1 Heat Flux and Inlet Temperature for SPSAH

Figure 3.1 shows the hourly variation of solar intensity versus local time of all the days when the experiments were done. The solar radiation was increasing from morning to a peak value at noon, and then it was decreasing in the afternoon until sunsets. The mean average values of solar radiation for the experiments of the 2, 4, and 6 fins SPSAHs were 755.9, 736 and 752.8 W/m^2 respectively. The measured solar intensities were stable throughout the days when the experiments were carried out. Fig. 3.2 shows the variation of the inlet temperature (i.e., ambient temperature) during the days when the experiments were performed. In general, the ambient temperature is found to be increasing slightly or fluctuating in some other days from morning until evening.

3.2 Temperature Rise through the Bed of SPSAH

The hourly temperature differences ($\Delta T = T_{out} - T_{in}$) at different mass flow rates for 2,4, and 6 fins SPSAHs are shown in Fig. 3.3, Fig 3.4 and 3.5 respectively. As

expected, for all cases, the value of ΔT increases in the morning to a peak value at noon and starts to decrease in the afternoon. For the configuration of the SPSAH which is used in this work, ΔT decreases with increasing air mass flow rate. The peak ΔT was achieved between 12:00 h and 13:00 h of the local time depending on the outdoor conditions such as solar intensity and wind speed. It is also found that the magnitude of ΔT was increased by increasing the number of fins for the same mass flow rate (Fig. 3.6). Moreover, it is found that the maximum average ΔT for the 6 fins SPSAH was higher if compared to 2 and 4 fins SPSAH for the same mass flow rates. The highest average and instantaneous peak ΔT obtained for the 6 fins SPSAH case were 36.88 ^{o}C and 51.1 ^{o}C respectively with mass flow rate of 0.0121 kg/s, while the average and the peak value ΔT obtained for maximum flow rate, m=0.042 were 19.69 and 28.45. The highest average and instantaneous peak ΔT obtained for the 4 fins SPSAH case were 34.85 ^{o}C and 49 ^{o}C respectively with mass flow rate of 0.0121 kg/s, while the average and the peak value ΔT obtained for maximum flow rate, m=0.042 were18.75 and 28. Finally the highest average and instantaneous peak ΔT obtained for the 2 fins SPSAH case were 32.31 ^{o}C and 44.2 ^{o}C respectively with mass flow rate of 0.0121 kg/s, while the average and the peak value ΔT obtained for maximum flow rate, m=0.042 were17.8 and 25.5.

As expected, there is a very strong correlation between the outlet temperatures from the SAH with the flux intensity. As the solar intensity changes, the outlet air temperature reacts to change similarly. Figure 3.1 shows the recorded hourly variation of solar intensity and fig 3.2 shows ambient temperatures vs. different standard local time during the tests for the SPSAH. Figures 3.3-3.5 show the temperature difference versus standard local time of the days at different mass flow rates for the SPSAH. Figure 3.6 shows the effect of number of fins on the ΔT.

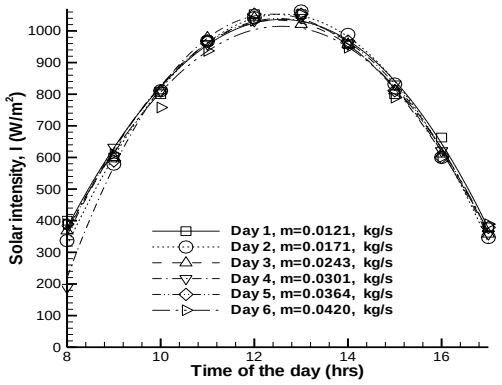

(a)

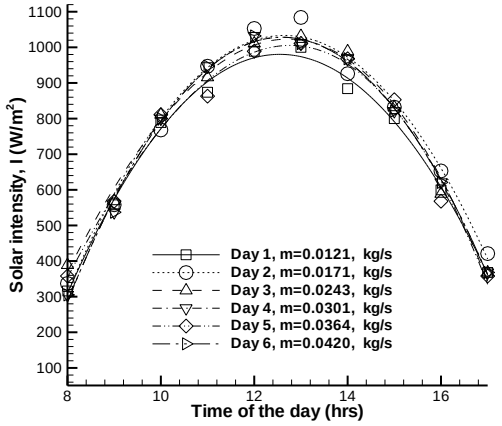

(b)

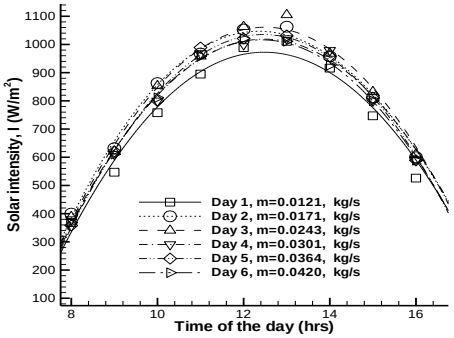

(c)

Figure 3.1: Hourly variation of solar intensity versus different standard local time of (a) 2 fins (b) 4 fins and (c) 6 fins for SPSAH

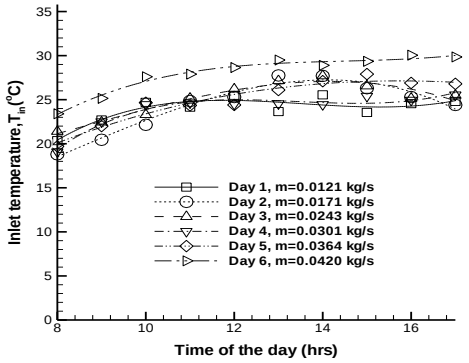

(a)

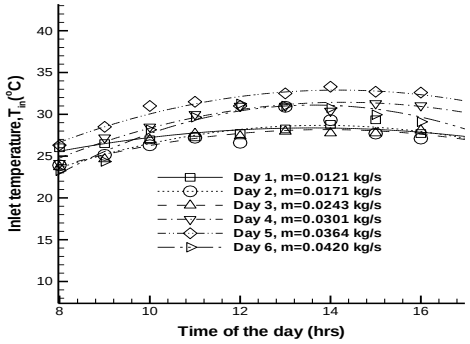

(b)

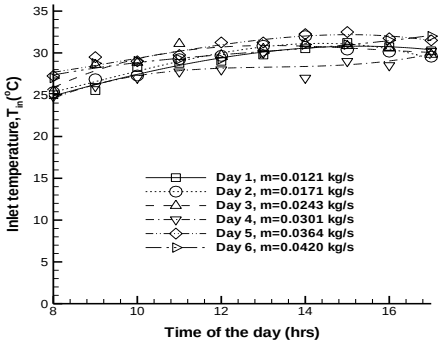

(c)

Figure 3.2: Ambient temperatures versus different standard local time of days for: (a) 2 fins (b) 4 fins and (c) 6 fins for SPSAH

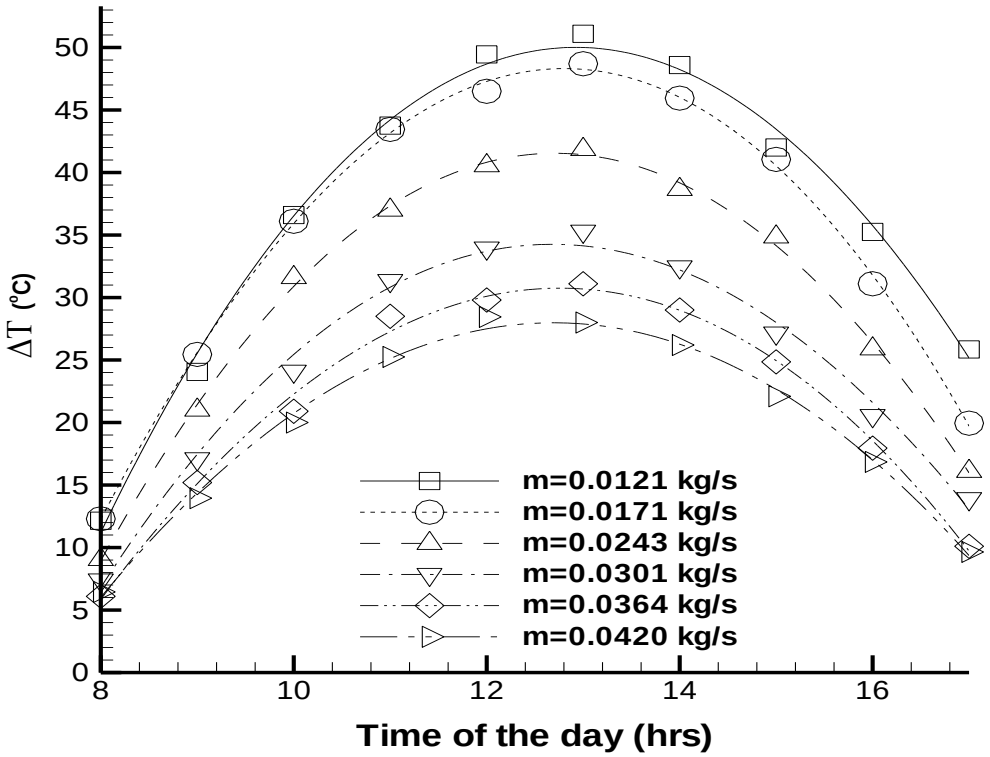

Figure 3.3: Temperature difference versus standard local time of the day at different mass flow rates for 2 fins SPSAH

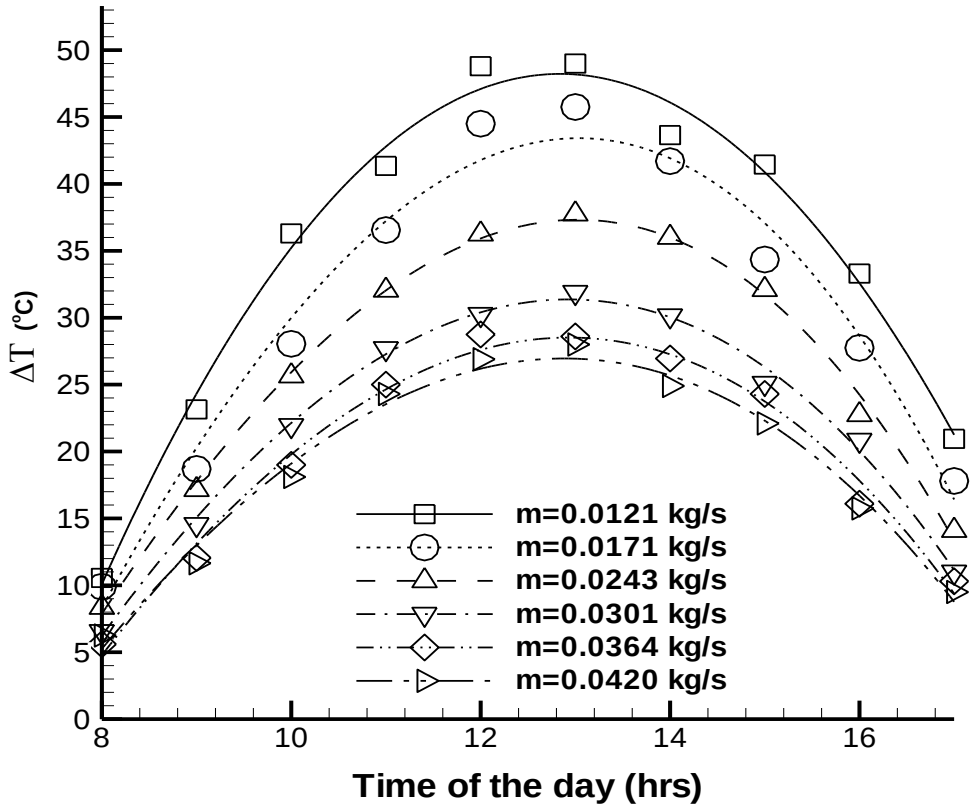

Figure 3.4: Temperature difference versus standard local time of the day at different mass flow rates for 4 fins SPSA.

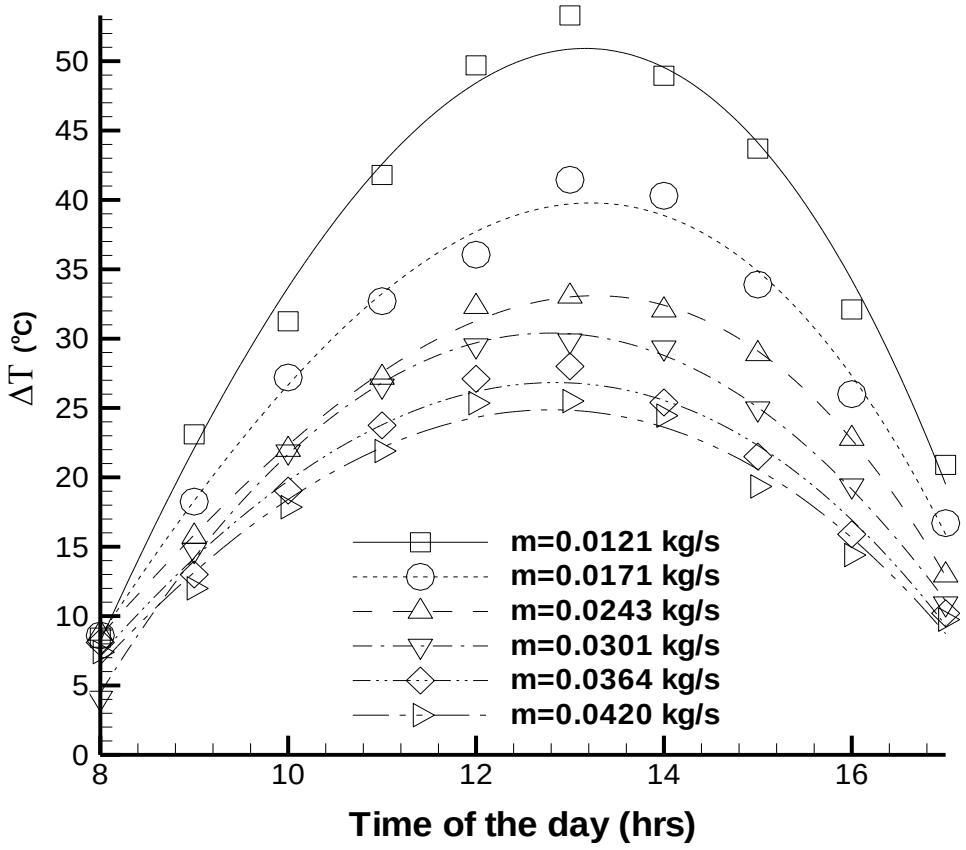

Figure 3.5: Temperature difference versus Standard local time of the day at different mass flow rates for 6 fins SPSAH

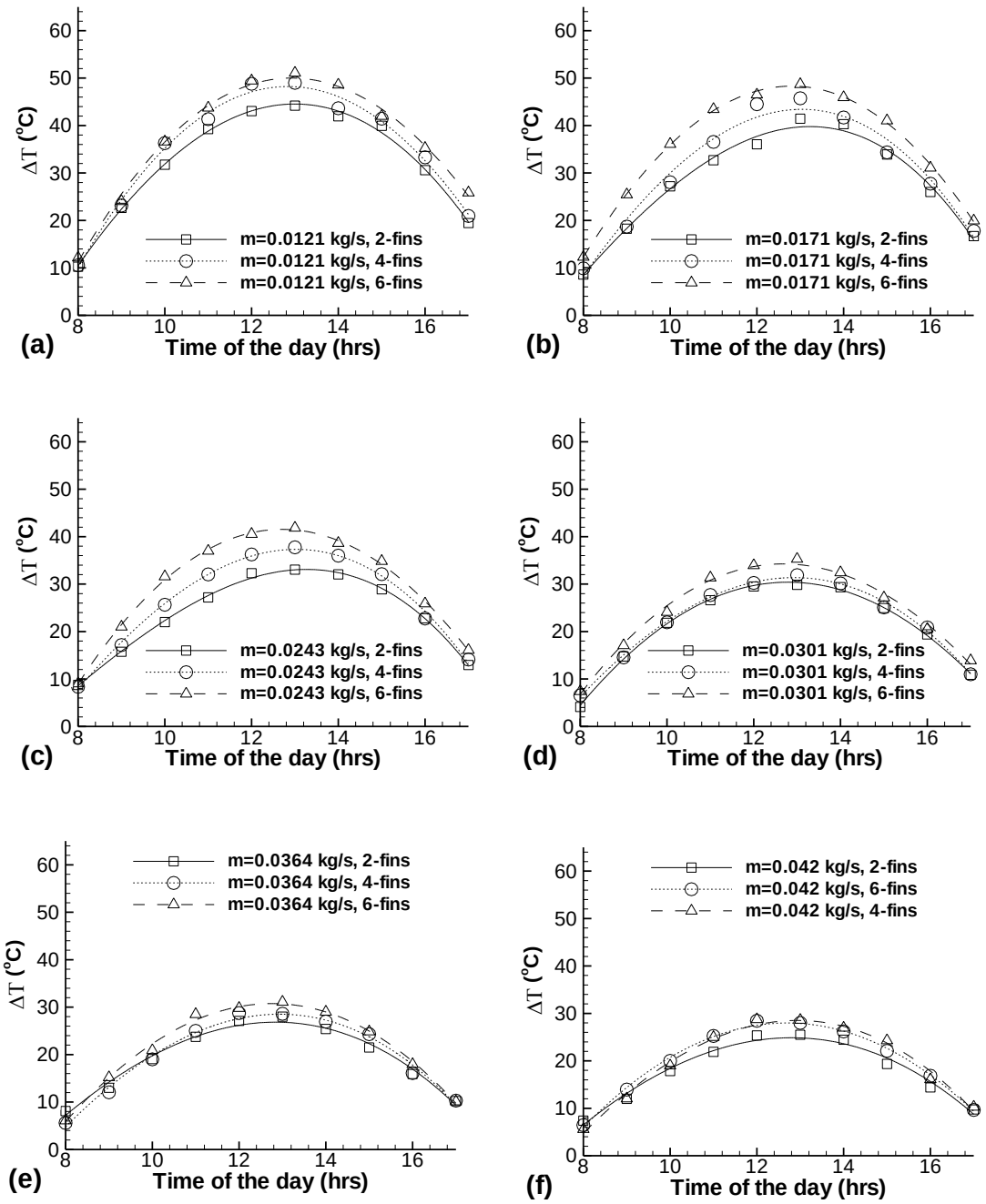

Figure 3.6: Effect of Number of Fins on the Temperature Difference at m (kg/s): a) 0.0121, b) 0.017, c) 0.0243, d) 0.0301 e) 0.0364 f) 0.042 in SPSAH

3.3 Efficiency of SPSAH

Efficiency versus time at different air mass flow rates for 2, 4 and 6 fins SPSAHs are presented in Figs 3.7-3.9. For the three types of SPSAHs investigated in this study, the thermal efficiency was increased by increasing the air mass flow rate for the same number of fins. The maximum efficiencies obtained from the 2, 4, and 6 fins SPSAHs were 71.80%, 74.91% and 79.81% respectively for the air mass flow rate of 0.042 kg/s. The efficiency of the SPSAH for most of the cases was found to be increasing from morning until afternoon. However, for high mass flow rate, there is a slight decreasing in the efficiency at afternoons. The increase in efficiency from morning until afternoon was due to the energy stored in the matrix bed. Whereas, energy stored in the matrix bed was decreased by increasing the mass flow rates thus, slight decrease in the efficiency in the afternoons was observed. The efficiency was always increased by increasing the number of fins (Fig. 3.10) for the same mass flow rate. Although in some days, there were some exceptions in the morning due to weather conditions.

The maximum average of daily efficiency for the 6, 4 and 2 fins SPSAH were 72.34%, 69.58 and 65.8% respectively with mass flow rate of 0.042 kg/s (Fig. 3.11). The average efficiency of the 6 fins collector was higher by 9.9%-21.1% than the 2 fins SPSAH. The 6 fins collector efficiency, depending on the air mass flow rate was higher by 4% up to 11% compared to the 4 fins SPSAH.

Finally the thermal efficiency of the 6 fins SPSAH was compared to some of the reported ones in the literature (Fig.3.12). It is found that, in the proposed model, the thermal efficiency is higher compared to the other models available in literature.

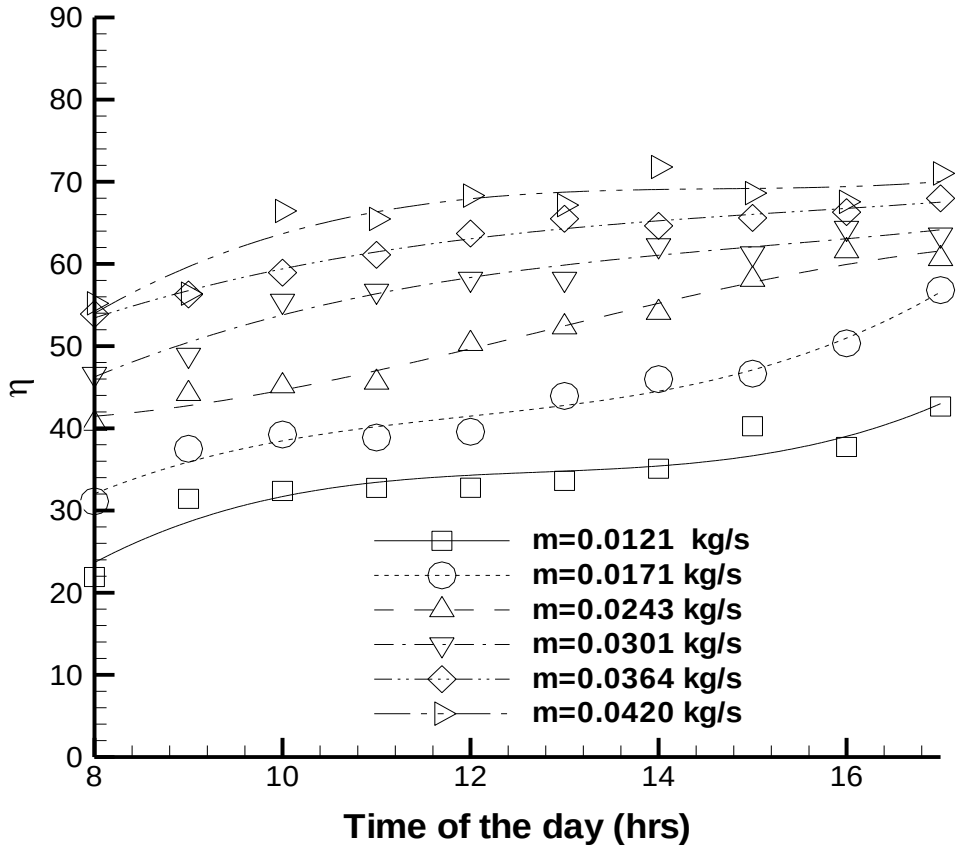

Figure 3.7: Variation of collector efficiency at different mass flow rates for 2-fins SPSAH

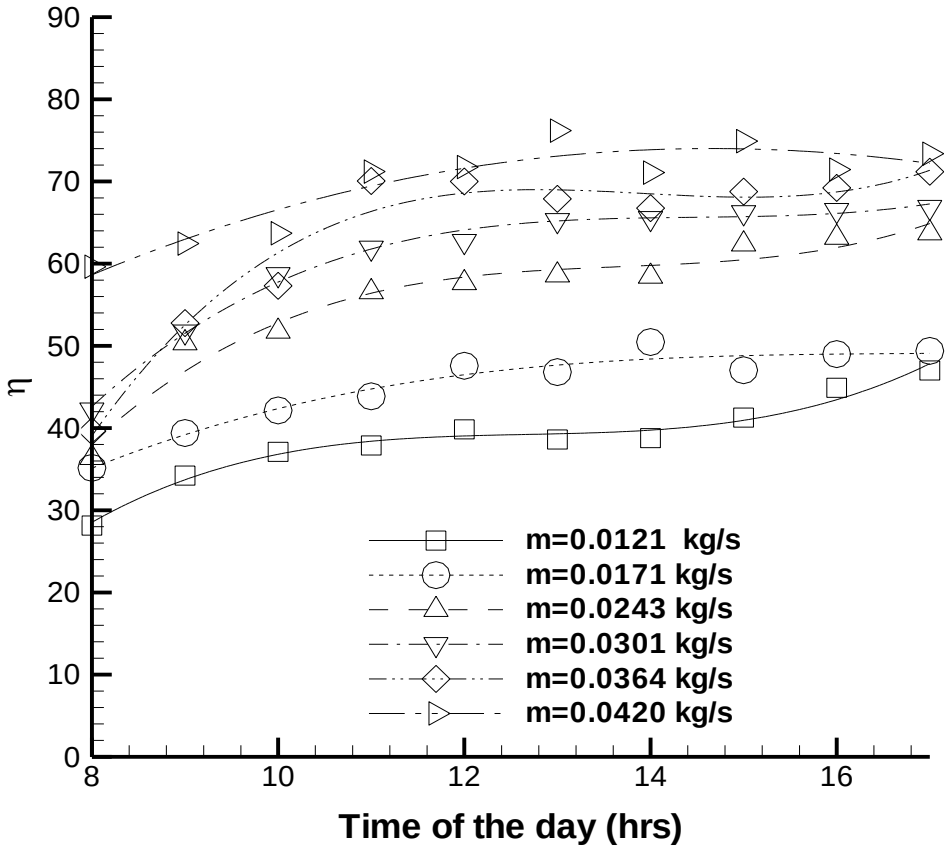

Figure 3.8: Variation of collector efficiency at different mass flow rates for 4-fins SPSAH

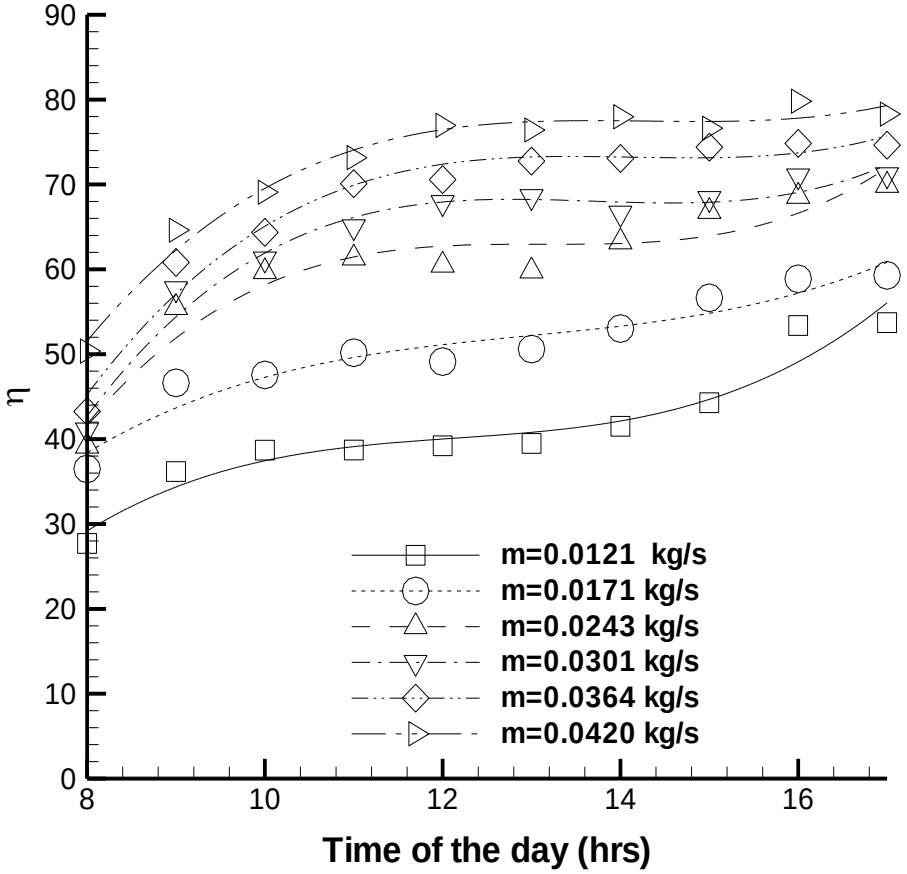

Figure 3.9: Variation of collector efficiency at different mass flow rates for 6-fins SPSAH

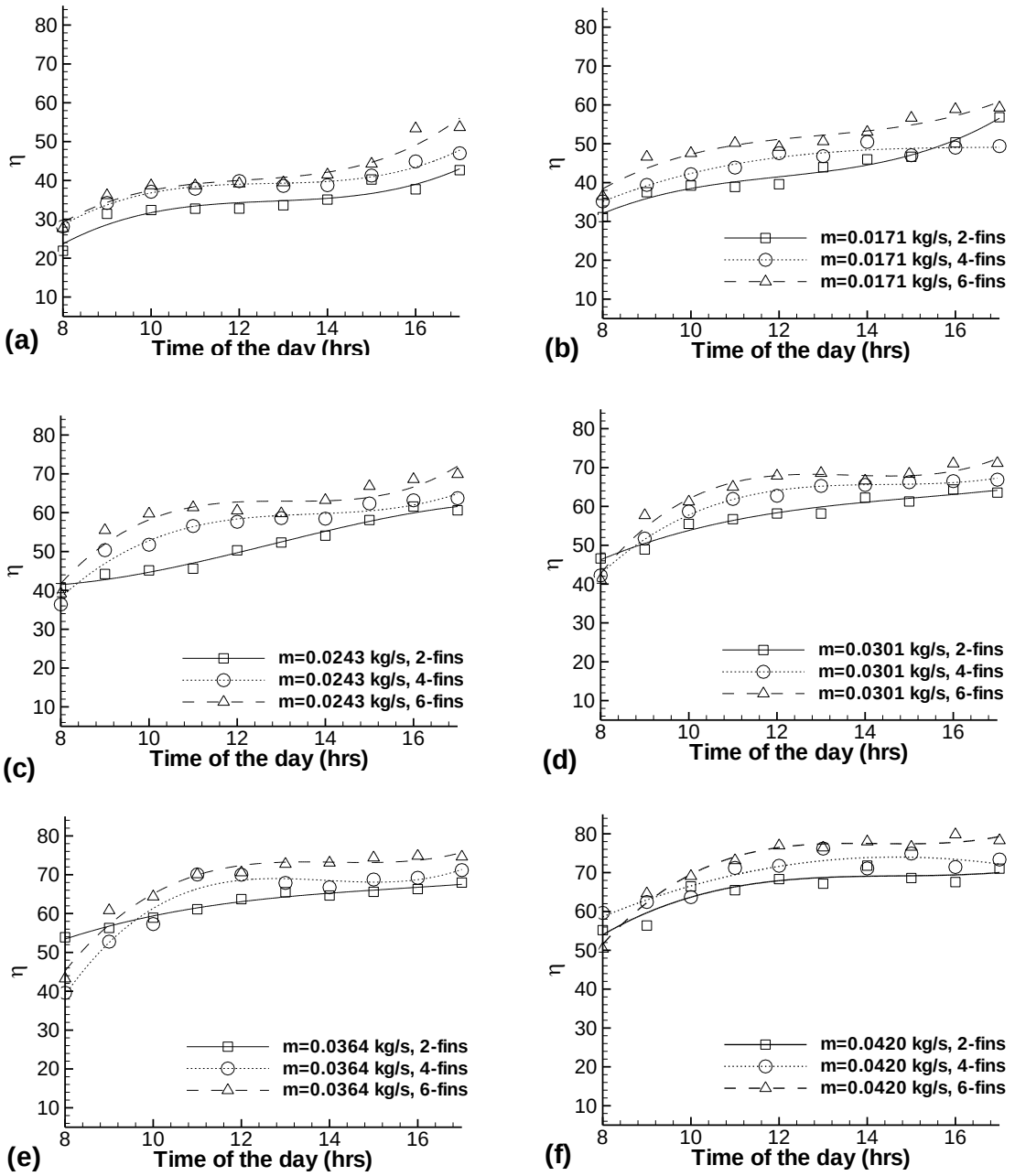

Figure 3.10: Effect of number of fins on the efficiency for mass flow rate m (kg/s) = a) 0.0121, b) 0.017, c) 0.0243, d) 0.0301 e) 0.0364 f) 0.042 for SPSAH

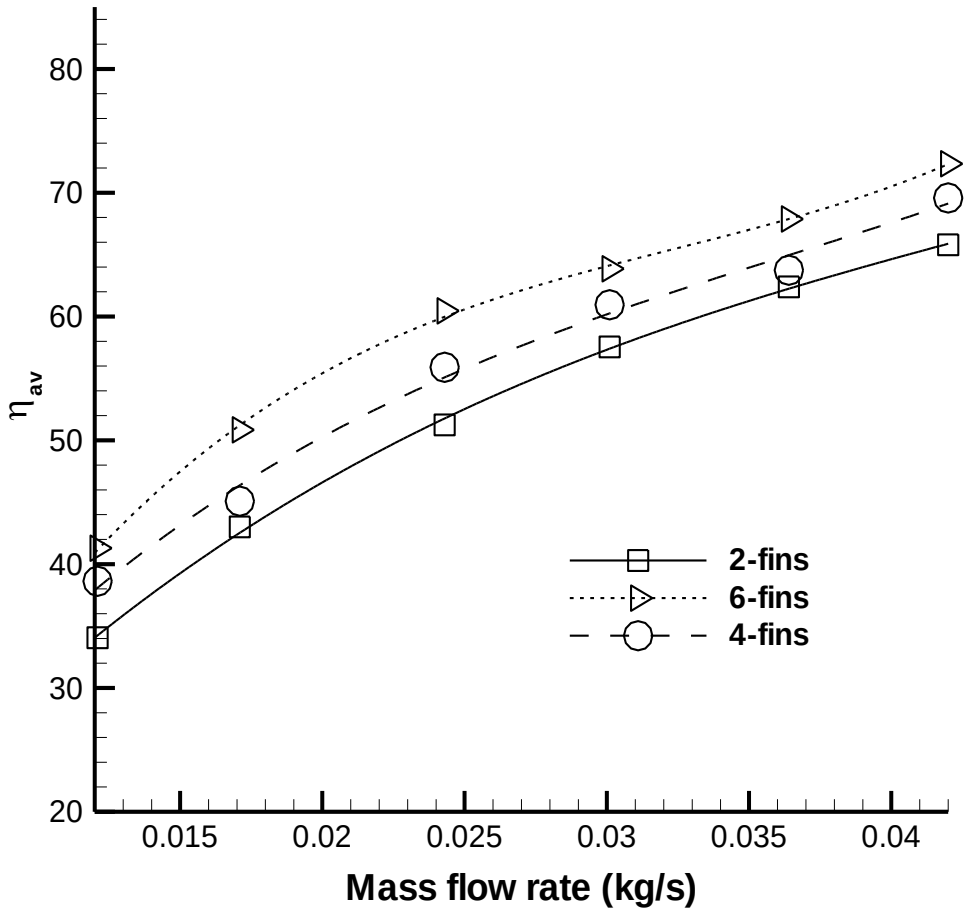

Figure 3.11: Average daily efficiency versus mass flow rate for 2, 4 and 6 fins SPSAH

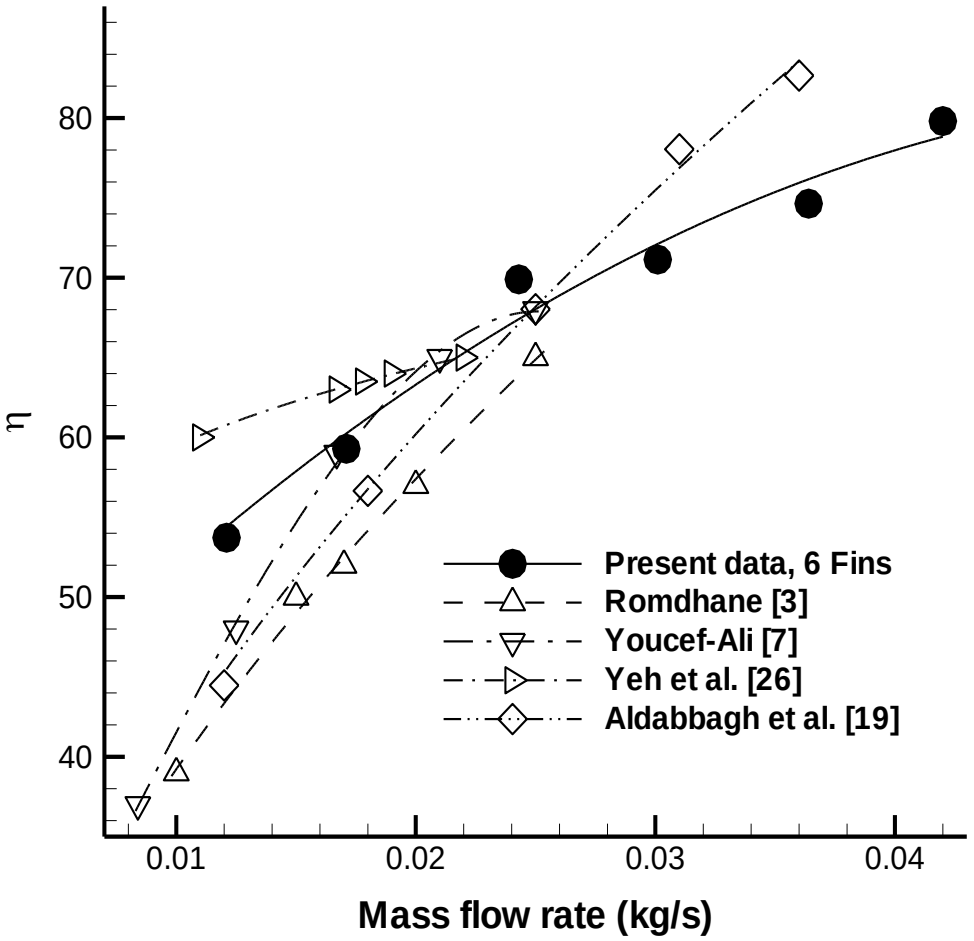

Figure 3.12: Efficiency comparison between the 6 fins SAH with some SAHs in literature.

3.4 Pressure Drop

The porous media increases the turbulence of flow and the contact surface area. The contact surface area increases the thermal performance of SAHs. On the other hand, using the porous media increases the pressure drop, so, it increases the power needed to operate the fan.

In this study, the pressure drop was between 10.5 Pa to 21.1 Pa for the 2, 4 and 6 fins with the minimum mass flow rate, m=0.0121 kg/s, and between 63.1 Pa and 77.9 Pa at maximum flow rate, m=0.042 kg/s, see Fig. 3.13. These values are quite acceptable and are within the limitations of the fan power needed for SAHs. The pressure drop in the proposed design was low because of two main reasons: First, increasing the porosity of the bed causes a decrease in the pressure drop where in these experiments the bed was designed with porosity more than 0.966. Secondly, the layers were organized in such a way to allow more smooth passage of airflow through the porous media (the layers of the wire mesh are parallel to the flow).

The pressure drop that is incurred as a result of using the new design does not present practical limitations on the use of the porous media for SAH. The improvement in the performance of the SAH is more than justified for the less overall significant increased pressure drop.

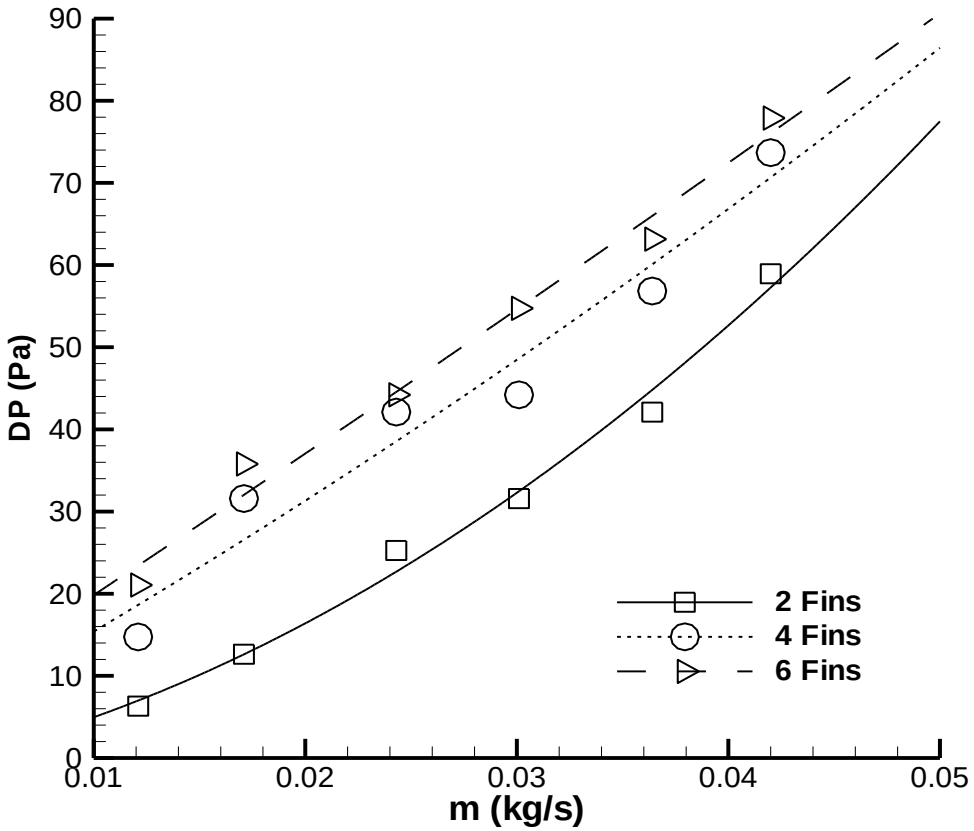

Figure 3.13: Pressure drop across the bed at different mass flow rates for SPSAH

Chapter 4

COUNTER PATH SOLAR AIR HEATER

As mentioned earlier in chapter one, the major heat losses from the collector are from the front cover (i.e., glazing), because the sides and the back of the collector are usually adequately insulated, while the front face must be exposed to solar radiation and exposed to the ambient temperature. The high temperature of the absorber plate, compared to the ambient temperature increases the driving force in the flow of heat in the cover direction; accordingly, the thermal losses increase. In the proposed CPSAH design, it is attempted to reduce heat losses to the ambient by forcing air to flow over the lower (inner) glass cover to preheat the air before passing over the absorber (i.e., layers of mesh wire). Therefore, energy extracted from the glass cover will be used to preheat the air. This arrangement requires two glass covers, or one glass cover and one plastic cover to reduce the cost (Fig.2.2). This arrangement forms what is called a counter flow heat exchanger.

This chapter deals with the results of experiments that were done to investigate the effect of partitioning counter flow wire mesh packed bed under Famagusta prevailing weather conditions during the summer months, 21.05.2010- 20.07.2010, with a clear sky condition. The experiments which were done in this chapter are in the same period of the SPSAH experiments. This means that the wind speed and relative humidity which were hourly recorded in SPSAH experiments are same for the CPSAH (i.e., the average mean values of the wind speed and relative humidity ratio are 5.1 m/s. and 67.24 % respectively).

4.1 Heat Flux and Inlet Temperature of CPSAH

Figure 4.1 shows the hourly variation of solar intensity versus local time of all the days when the experiments were done. The average values of solar radiation for the experiments of the 2, 4, and 6 fins CPSAH were 730.26, 721.18 and 736 W/m^2 respectively. The measured solar intensities were stable throughout the days when the experiments were carried out except on the 6^{th} day of the two fins case where the weather was partially cloudy in the morning.

Figure 4.2 shows the variation of the inlet temperature (i.e., ambient temperature). For the configuration of the CPSAH which is used in this work, ΔT decreases with increasing air mass flow. Figures 4.3-4.5 show the hourly temperature difference (ΔT) at different mass flow rates for 2, 4, and 6 fins CPSAHs. It is also found that the magnitude ΔT increased by increasing the number of fins for the same mass flow rate (Fig 4.6). The peak ΔT was achieved between 12:00 h and 13:00 h. The ΔT for the 6 fins CPSAH was the highest compared to 2 and 4 fins CPSAH for the same mass flow rates. The highest average and instantaneous peak ΔT obtained from this work were 43.1 ^oC and 62.1 ^oC respectively for the 6 fins CPSAH with mass flow rate of 0.0121 kg/s.

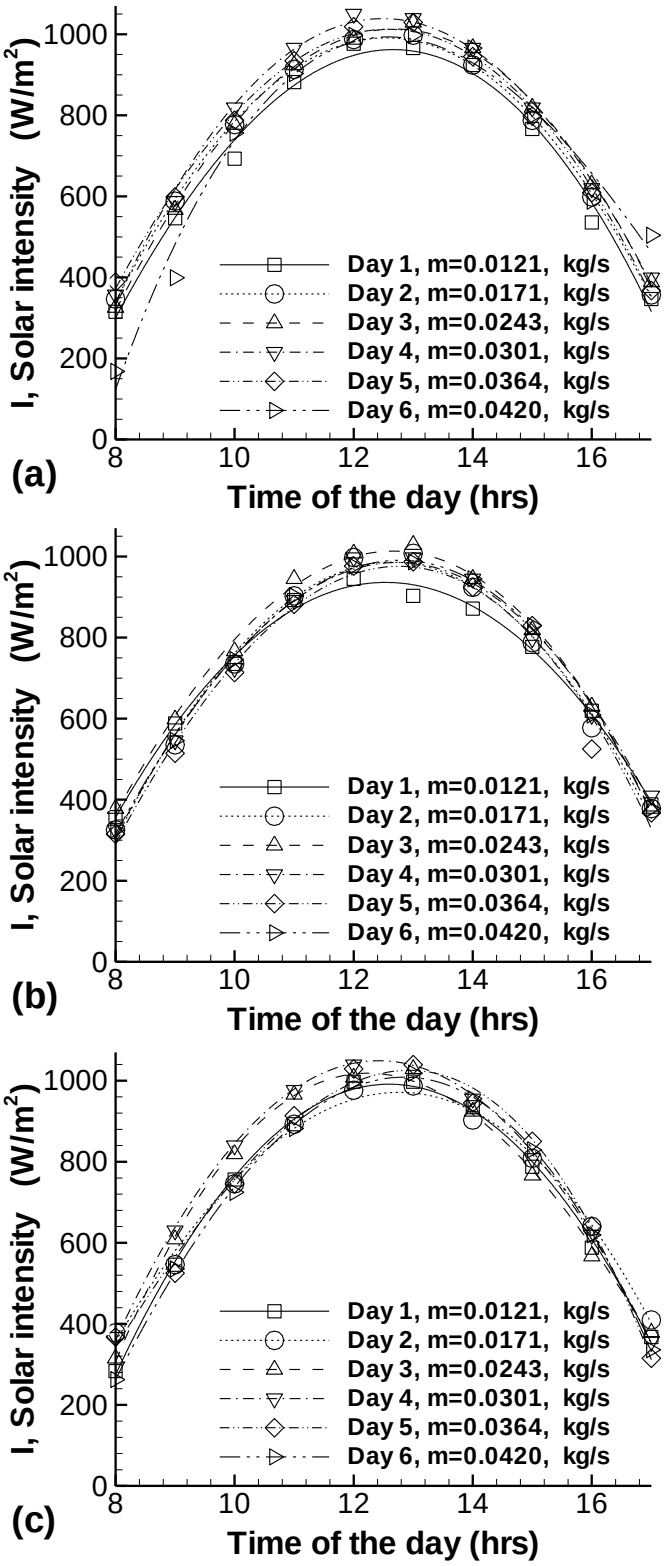

Figure 4.1: Hourly variation of solar intensity versus different standard local time of (a) 2 fins (b) 4 fins and (c) 6 fins CPSAH

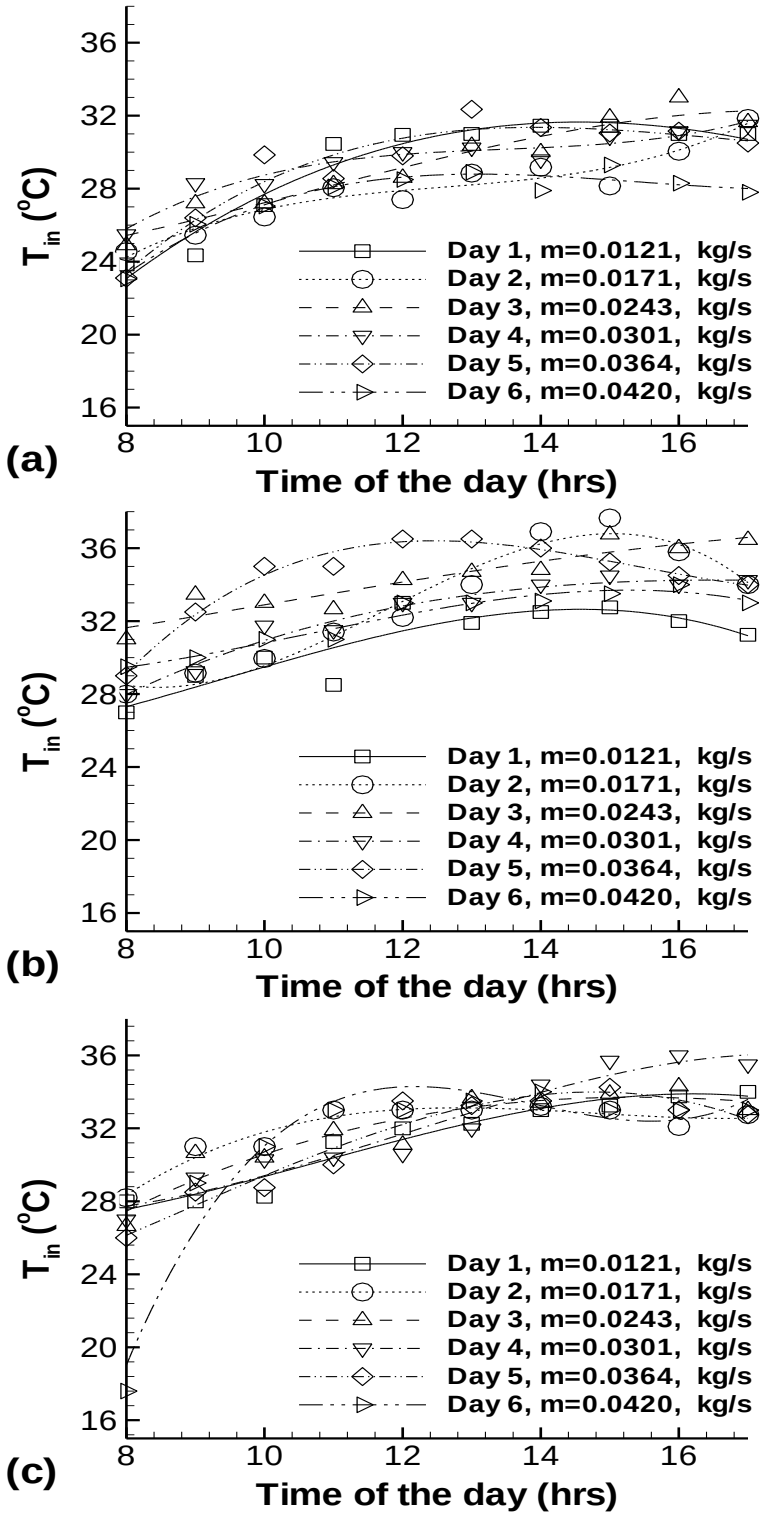

Figure 4.2: Ambient temperatures versus different standard local time of days for: (a) 2 fins (b) 4 fins and (c) 6 fins CPSAH

4.2 Temperature Rise Through the Bed of CRASH

From the literature review, the maximum temperature difference recorded by Esen (2008) was about 23.0 ^{o}C at solar radiation of 880 W/m^2 and mass flow rate of 0.02 kg/s. Sopian et al. (2007) reported that the maximum temperature difference was 40 ^{0}C for the solar intensity of 950 W/m^2 with air mass flow rate of 0.0995 kg/s by using double path SAH. Romdhane et al. (2007) investigated experimentally and theoretically a double-glass double path solar air heater with a packed bed above the heater absorber plate. They reported that the maximum ΔT was 35.0 ^{o}C at solar intensity 850 W/m^2 and mass flow rate of air was 0.0105 kg/s. El-Sebaii et al. (2007) reported that the maximum value of ΔT is 48.0 ^{o}C when iron scraps were used as packed bed above the absorber plate and 39.0 ^{o}C for gravel if it is used as a packed bed for the air mass flow rate 0.0105 kg/s and solar intensity 850 W/m^2.

4.3 Efficiency of CPSAH

Figures 4.7-4.9 show the variation of collector efficiency at different mass flow rates for the three types of CPSAHs investigated in this study as the thermal efficiency increases with the standard local time of the day from morning until evening. The maximum efficiencies obtained from the 2, 4, 6 fins CPSAHs were 75.0%, 82.1% and 85.9% respectively for the air mass flow rate of 0.042 kg/s. Figure 4.10 and Fig. 4.11 show that The efficiency was increased with increasing the number of fins for the same mass flow rate. The increase in efficiency was due to the increase in the air velocity in the path between the fins. The velocity in between the fins increased with increasing the number of fins as a result of increase in the path length for the same mass flow rate (Table 4-1).

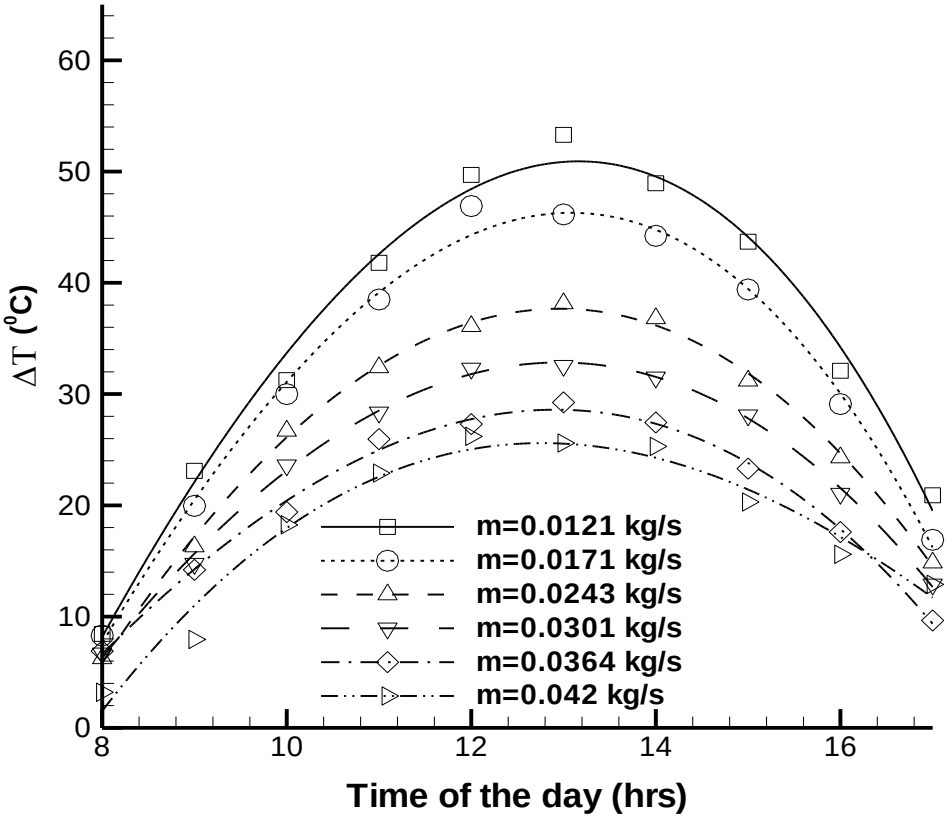

Figure 4.3: Temperature difference versus standard local time of the day at different mass flow rates for 2-fins CPSAH

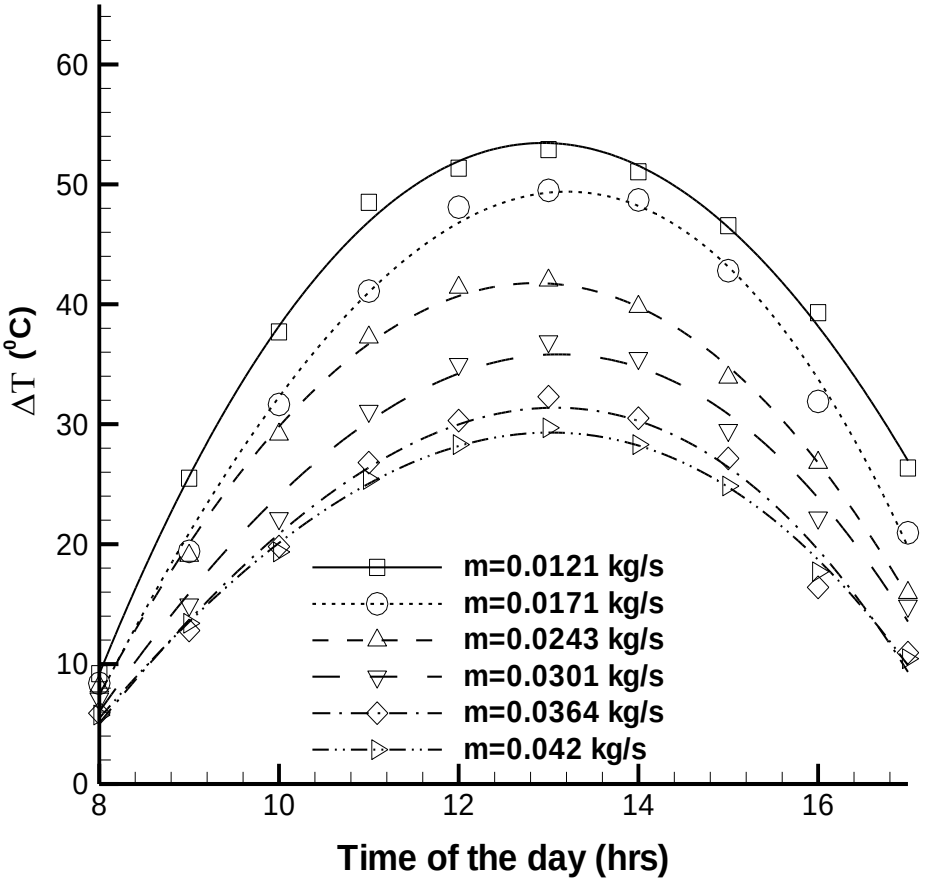

Figure 4.4: Temperature difference versus standard local time of the day at different mass flow rates for 4-fins CPSAH

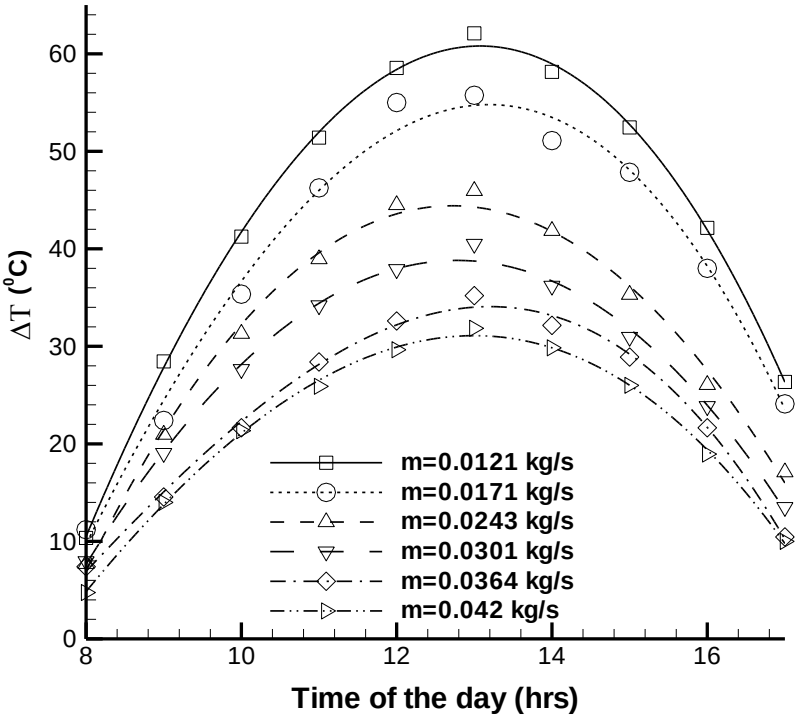

Figure 4.5: Temperature difference versus standard local time of the day at different mass flow rates for 6-fins CPSAH

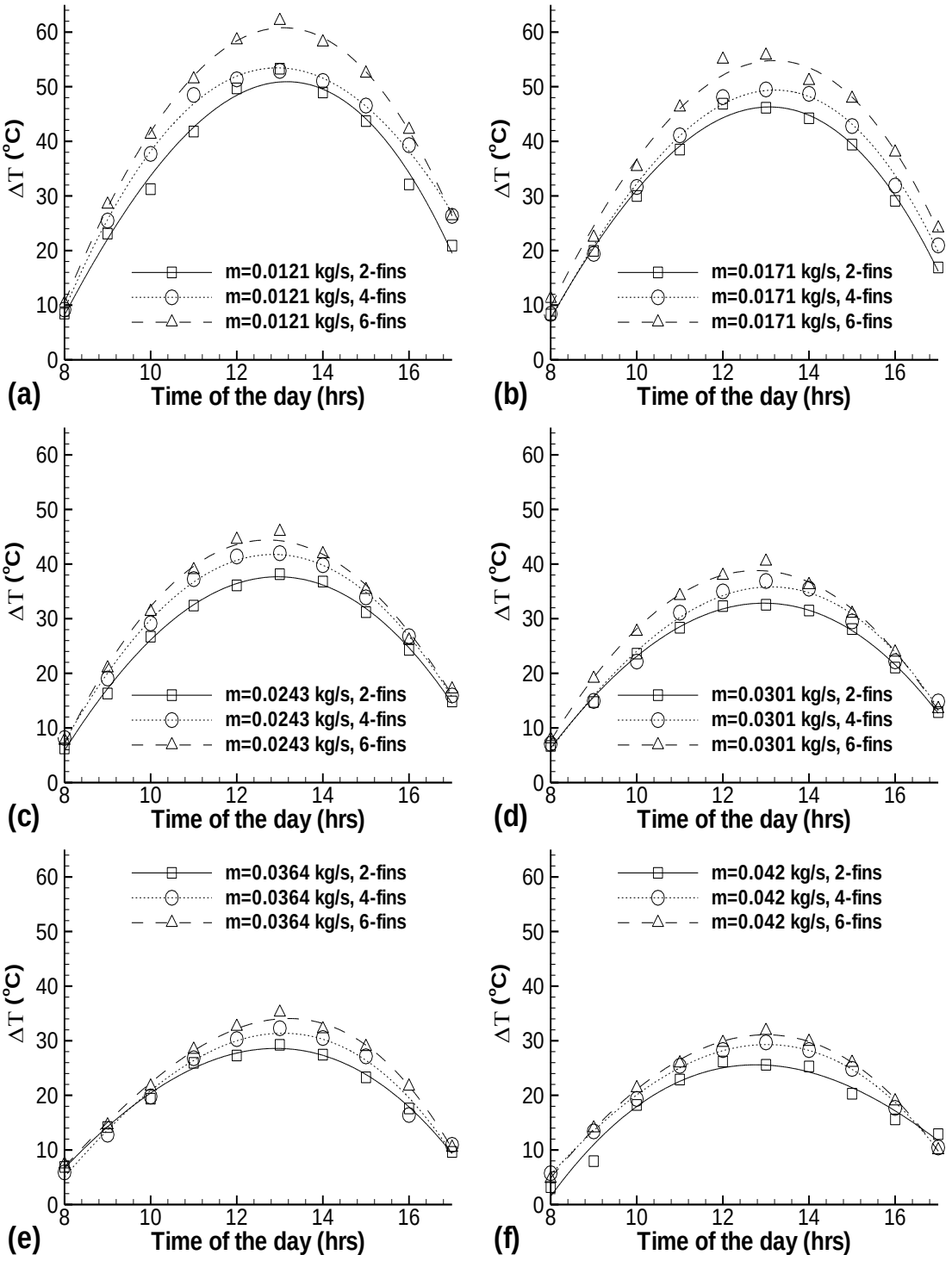

Figure 4.6: Effect of number of fins on the temperature difference at m (kg/s) = a) 0.0121, b) 0.017, c) 0.0243, d) 0.0301 e) 0.0364 f) 0.042 for CPSAH

As mentioned earlier, Ozgen et al. (2009) argued that the collector efficiency increased substantially when the fluid velocity was increased. Moreover, it is obvious that the path length of the 6 fins SAH is more than the 2 fins, hence the air will carry more heat from the bed.

Recently, Aldabbagh et al. (2010) , Omojaro and Aldabbagh (2010), Aldabbagh et al. (2010) found that the efficiency increases to the maximum value at 12:00-13:00 hrs, and then starts to decrease later on in the afternoon. However, our observations are not similar (Figs. 4.7 - 4.9). This is due to the change of the number of wire mesh layers in the matrices which affects the porosity of the bed. Increasing the number of layers (decreasing porosity) means increasing the contact surface area in SAH. Parasad et.al. (2009) found that efficiency increased significantly by increasing the number of wire mesh. The maximum average daily efficiencies for the 6, 4, and 2 fins CPSAH weere 79.5%, 75.3% and 68.9% respectively with mass flow rate of 0.042 kg/s (Fig.4.12). The average efficiency of the 6 fins collector was higher by 5.6%-10.5% and by 15.4 % 19.1 % than the 4 fins and 2 fins SAHs respectively depending on the air mass flow rate.

The comparison of the thermal performance of the six fins SAH with other SAHs reported in the literature is presented in Fig. 4.13. It is clear that the proposed 6 fins SAH has higher efficiency than the published data.

4.4 Pressure Drop In CPSAH

In this study the pressure drop is calculated to be in between 14 Pa to 23.8 Pa for the 2 and 6 fins respectively with the minimum mass flow rate (m=0.0121 kg/s), and between 68.7 Pa and 84.5 Pa at maximum flow rate m=0.042 kg/s (Fig. 4.14). The new proposed design of the porous matrices in CPSAHs minimizes the pressure drop

compared to the finned SAH mentioned in literature. Romdhane (2007) found that the pressure drop in his proposed design was between 20 Pa and 65 Pa at mass flow rate 0.0057 kg/s while, the pressure drop was between 50 Pa and 170 Pa at mass flow rate 0.0072 kg/s in the transversal wrinkled baffles and the mixed transversal-longitudinal baffles arrangements.

4.5 Energy Stored In SAH

As mentioned earlier, the efficiency of the solar air heater used to increase in the afternoon. This increase is due to the stored energy in the bed. The increase in efficiency is more clear when the mass flow rate through the bed is low, Figs. 3.7–3.9 and Fig. 4-7 up to Fig. 4-9. To study the heat storage in the bed and to find its amount, the experiment was run during one complete day from 07:00hrs to 20:30hrs until the outlet temperature of air flow was nearly equal to the inlet temperature (Fig 4.15). The stored energy in the SAH during the period of sunshine was used up in 3.5 hours after the sunset.

4.6 Performance Comparison Between SPSAH and CPSAH

The main heat losses from the SAHs is from the upper part through the glass cover. To reduce these losses, the CPSAH was introduced and discussed at the beginning of this chapter. In this section the performance of the CPSAH will be compared to the SPSAH.

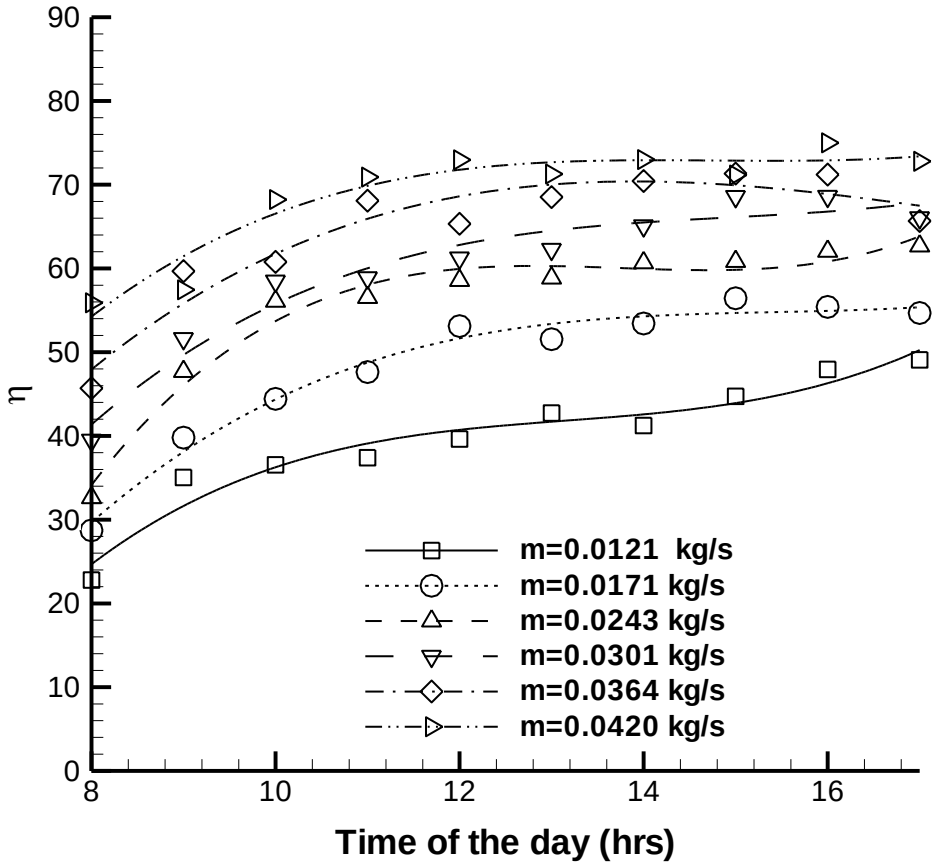

Figure 4.7: Variation of collector efficiency at different mass flow rates for 2-fins CPSAH

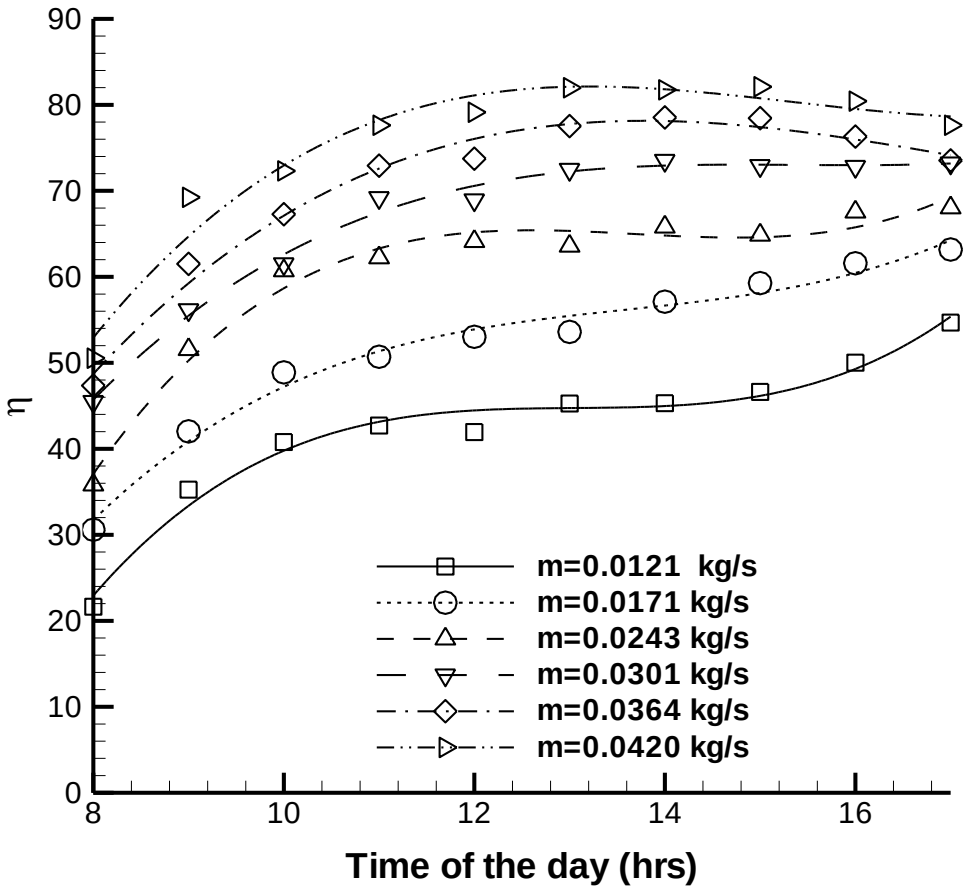

Figure 4.8: Variation of collector efficiency at different mass flow rates for 4-fins CPSAH

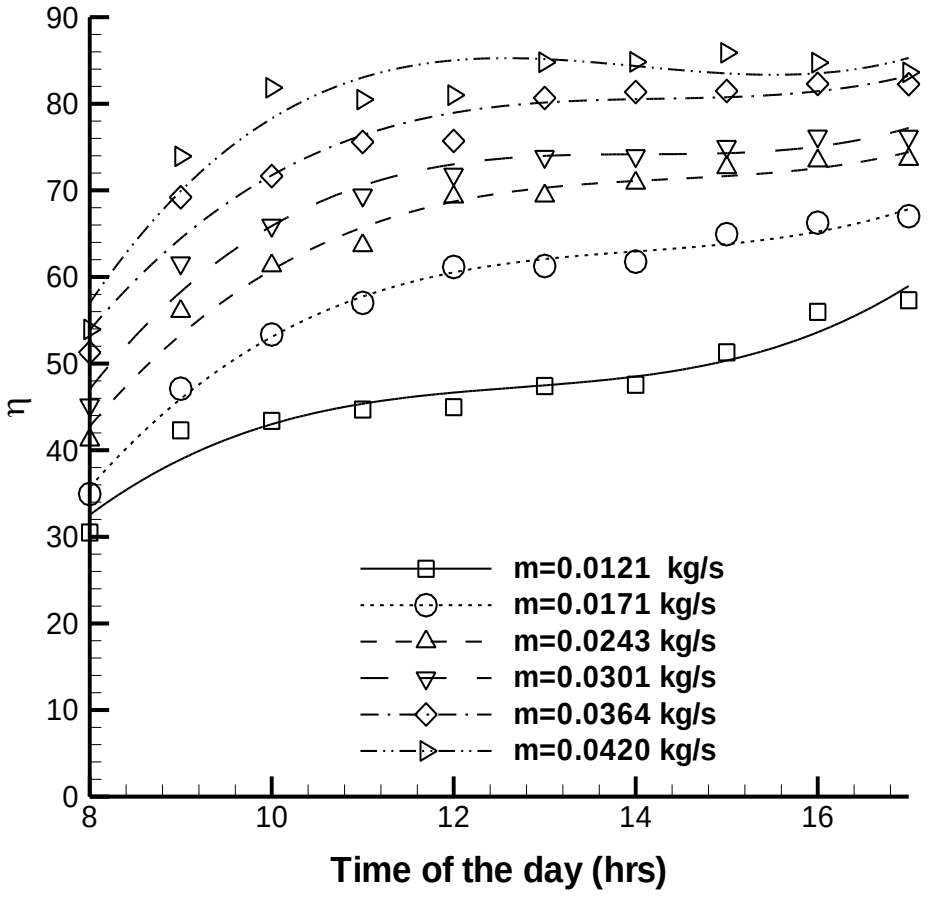

Fig. 4.9 Variation of collector efficiency at different mass flow rates for 6-fins CPSAH

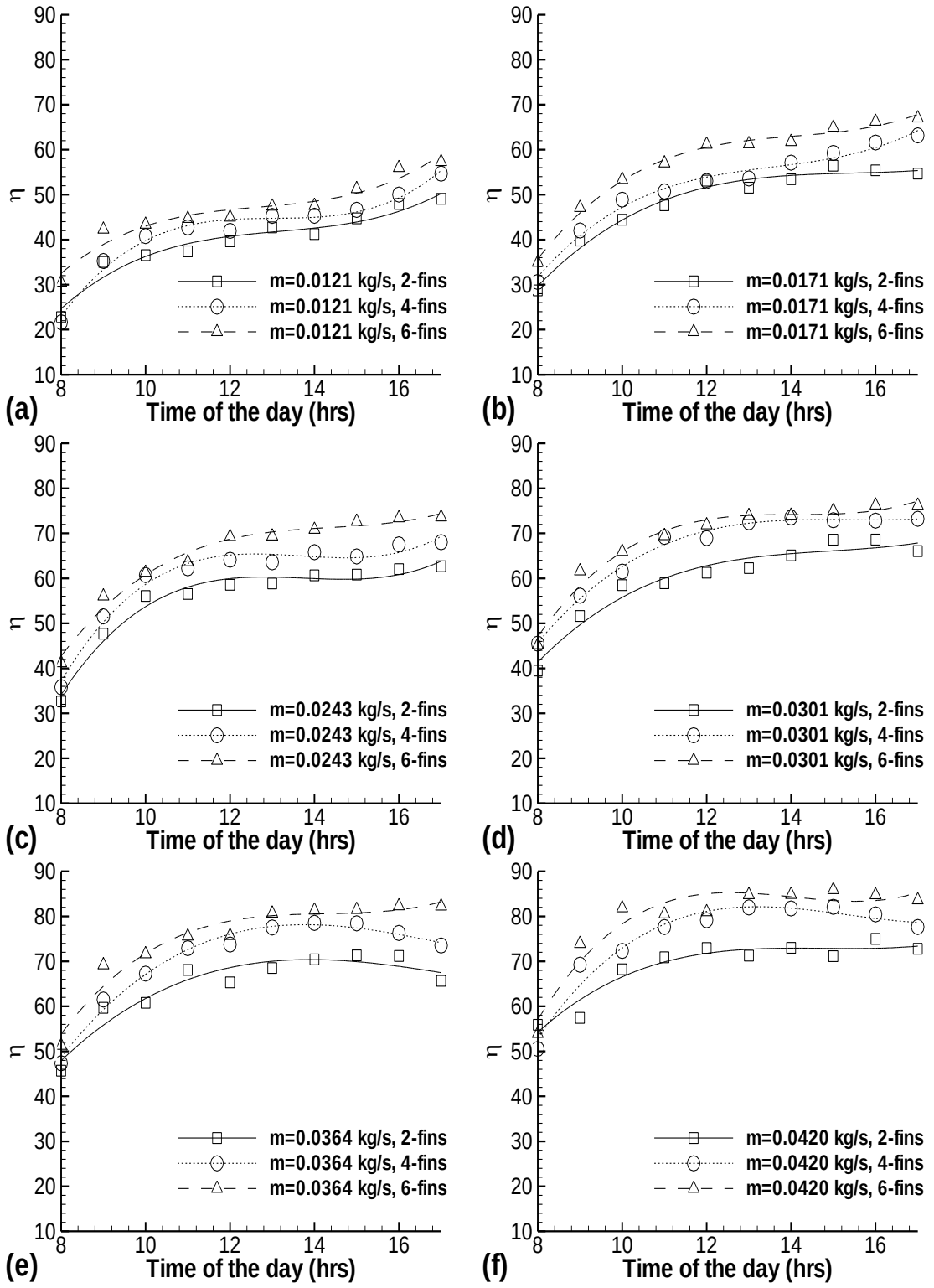

Figure 4.10 Effect of number of fins on the efficiency for mass flow rate m (kg/s) = a) 0.0121, b) 0.017, c) 0.0243, d) 0.0301 e) 0.0364 f) 0.042 for CPSAH

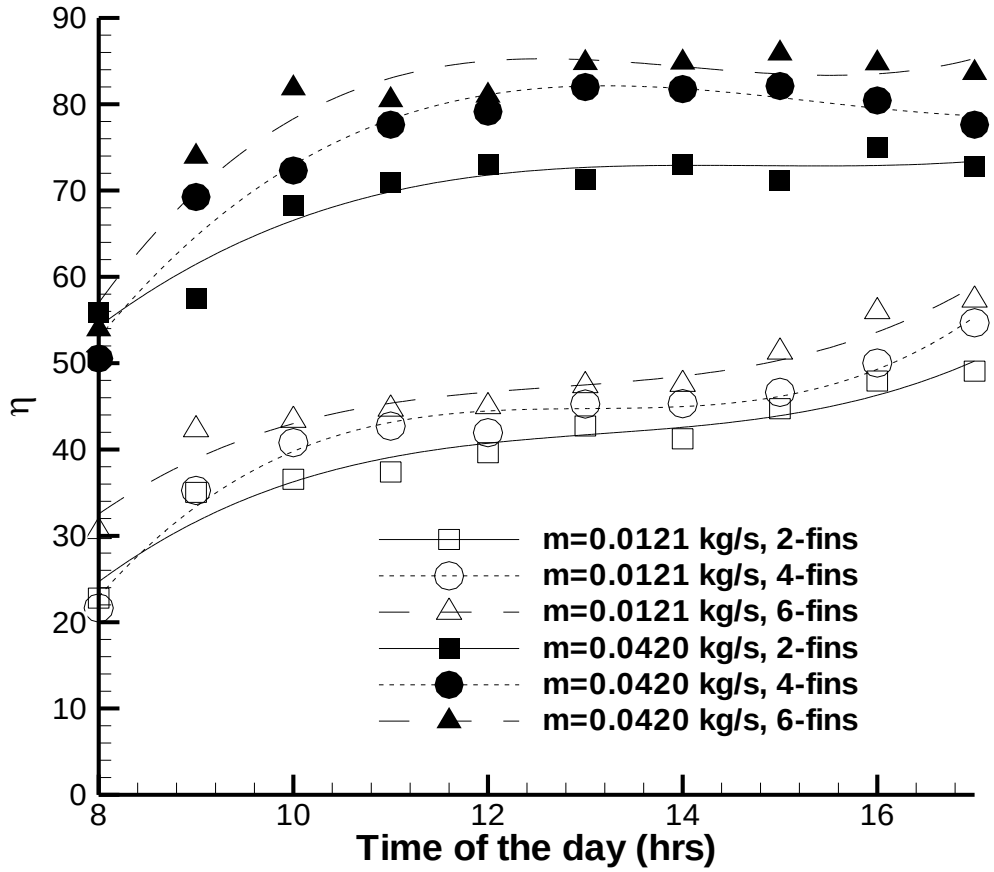

Figure 4.11: Effect of number of fins on the efficiency for minimum and maximum mass flow rate (0.0121, 0.042 kg/s) for CPSAH

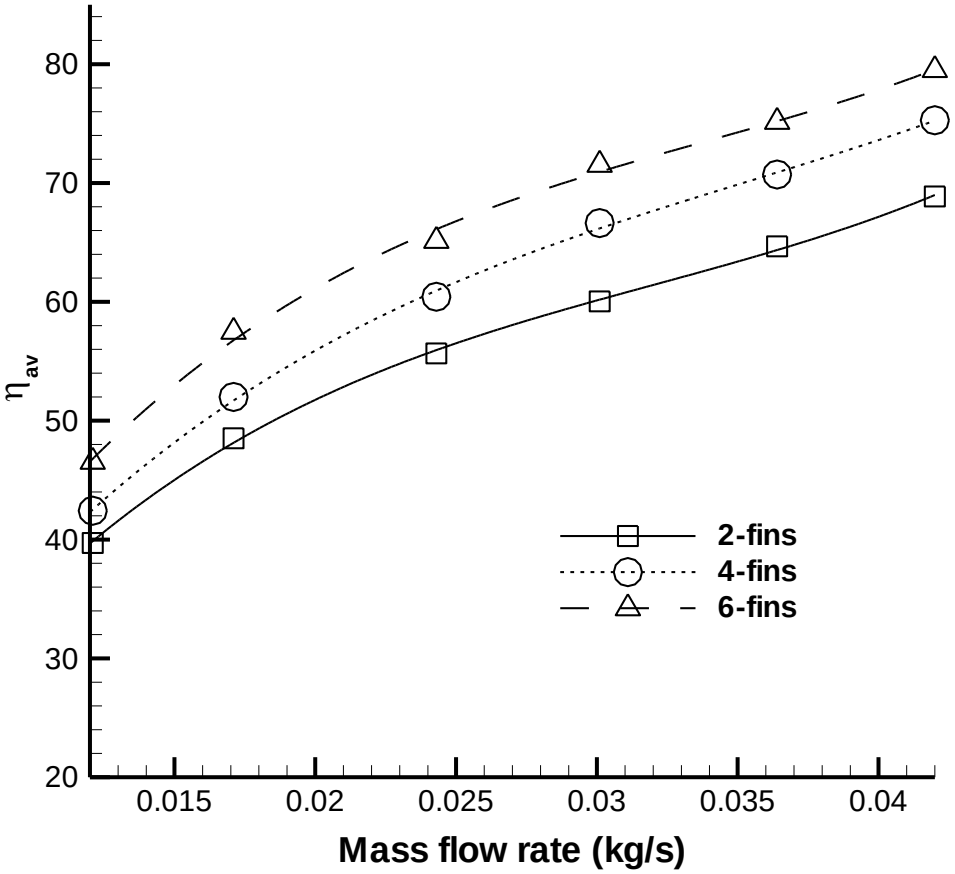

Figure 4.12: Average daily efficiency versus mass flow rate for 2, 4 and 6 fins CPSAH

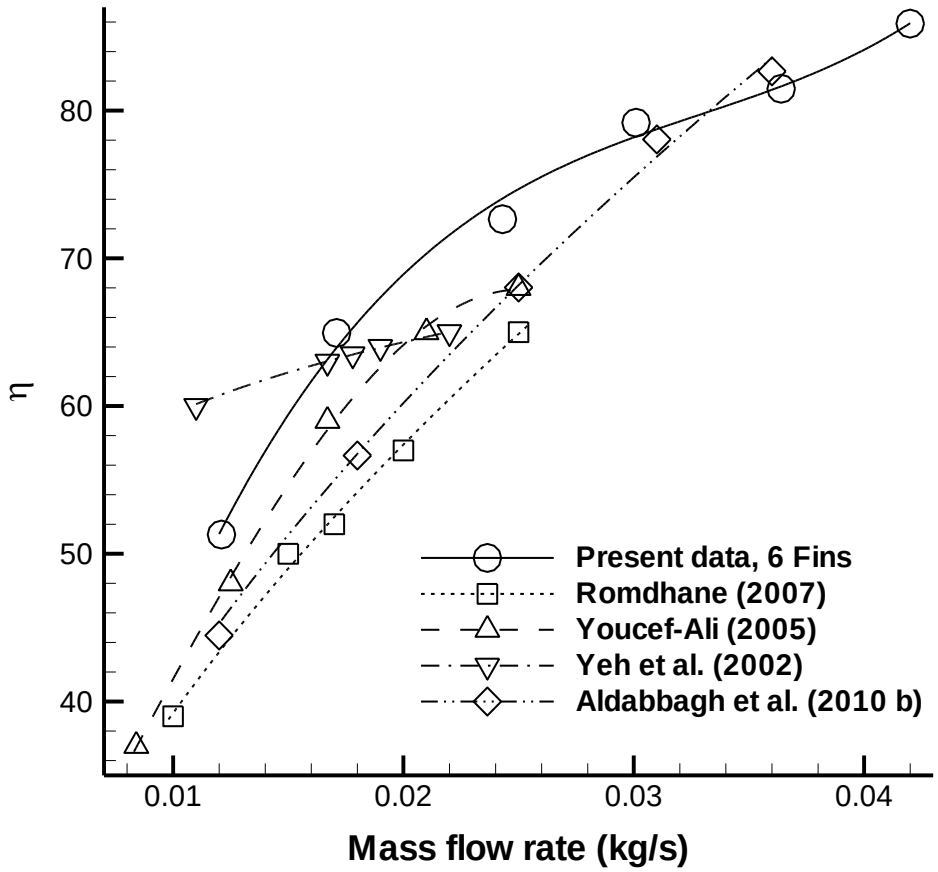

Figure 4.13: Comparison of efficiency between the proposed CPSAH with ones in the literature

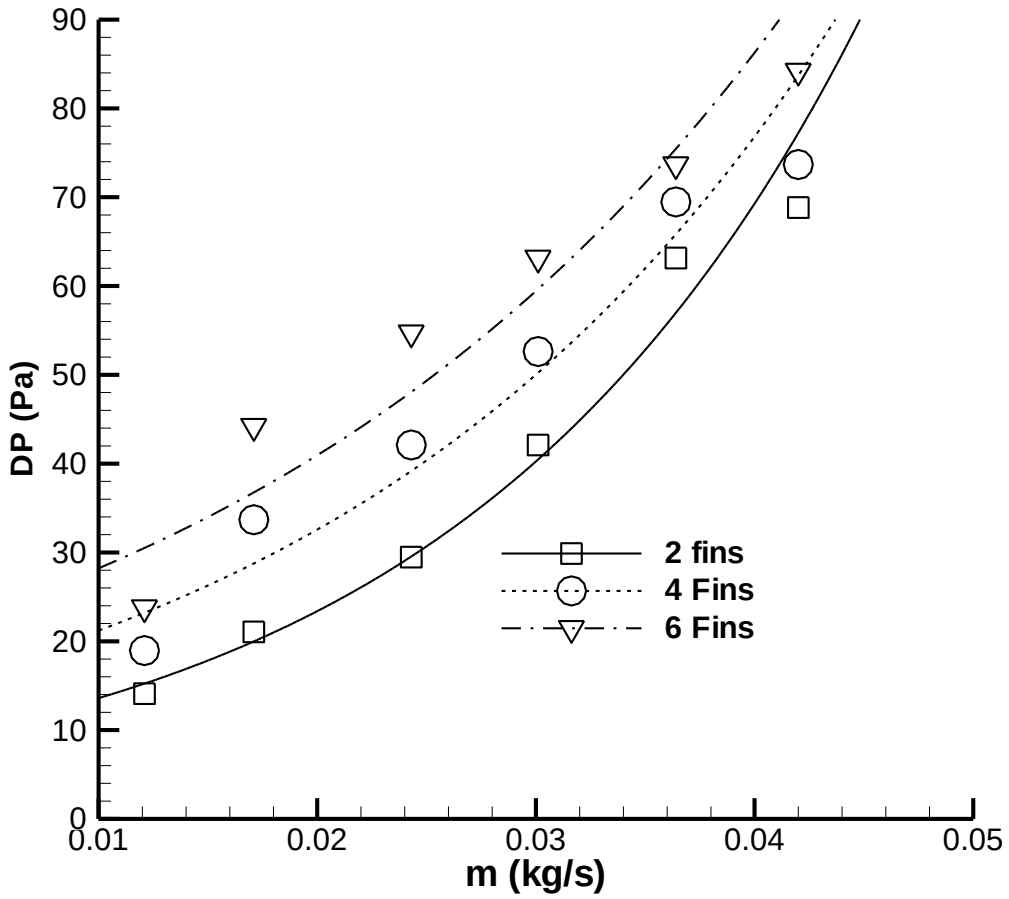

Figure 4.14: Pressure drop across the bed at different mass flow rates for CPSAH

4.6.1 Outlet Air Temperature Difference Comparison

Figures 4.16-4.18 compare the bulk temperature difference of passing air across the bed (ΔT) of SPSAH and CPSAH at different time of a day. It is clear that the outlet temperature difference (ΔT) of the CPSAH is always higher than the SPSAH during the sunshine hours regardless the number of fins used in the SAH. In some days there are some exceptions especially in the morning at 08:00hrs when the value of ΔT for SPSAH is equal to, or less than the CPSAH. These cases are clear in the previously presented Figs 4.16 - 4.18. The main reason was the low solar radiation. As the mesh wire layers are closer to the upper glazing in the SPSAH they receive more radiation early in the morning compared to the CPSAH. Also low temperatures in the SAHs in the morning means heat losses were also low, so, the ΔT were almost equal.

However, the number of fins affects the difference in magnitude of the increment in ΔT between SPSAH and CPSAH. It is obvious that as the number of fins increases the difference in output temperature between SPSAH and CPSAH also increases for the same mass flow rates. On the other hand, as the mass flow rate increases, the difference of ΔT between the CPSAH and SPSAH decreases for constant number of fins (Fig.4-18). The main reason is that as the mass flow rate increases the heat losses through the glazing decreases especially in the SPSAH due to the higher velocity of the working fluid in the collector. The bed temperature is kept at lower value ΔT_b for higher mass flow rate so the driving force of heat loss will be less. This will be discussed in detail in the following section. Table 4-2 summarizes the difference of bulk temperature of air passing through the bed (ΔT) of SPSAH and CPSAH. Table 4-3 shows the maximum and average ΔT obtained for SPSAH and CPSAH for different number of fins and mass flow rates.

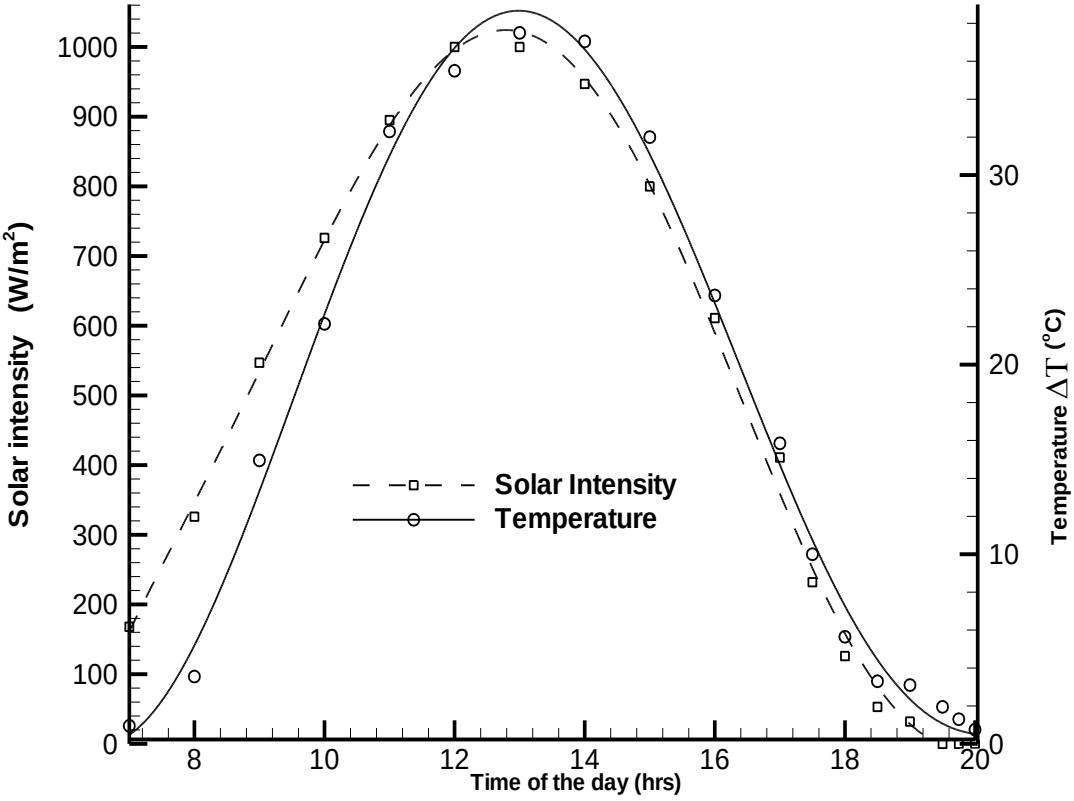

Figure 4.15: Solar intensity and temperature difference for one complete day for CPSAH

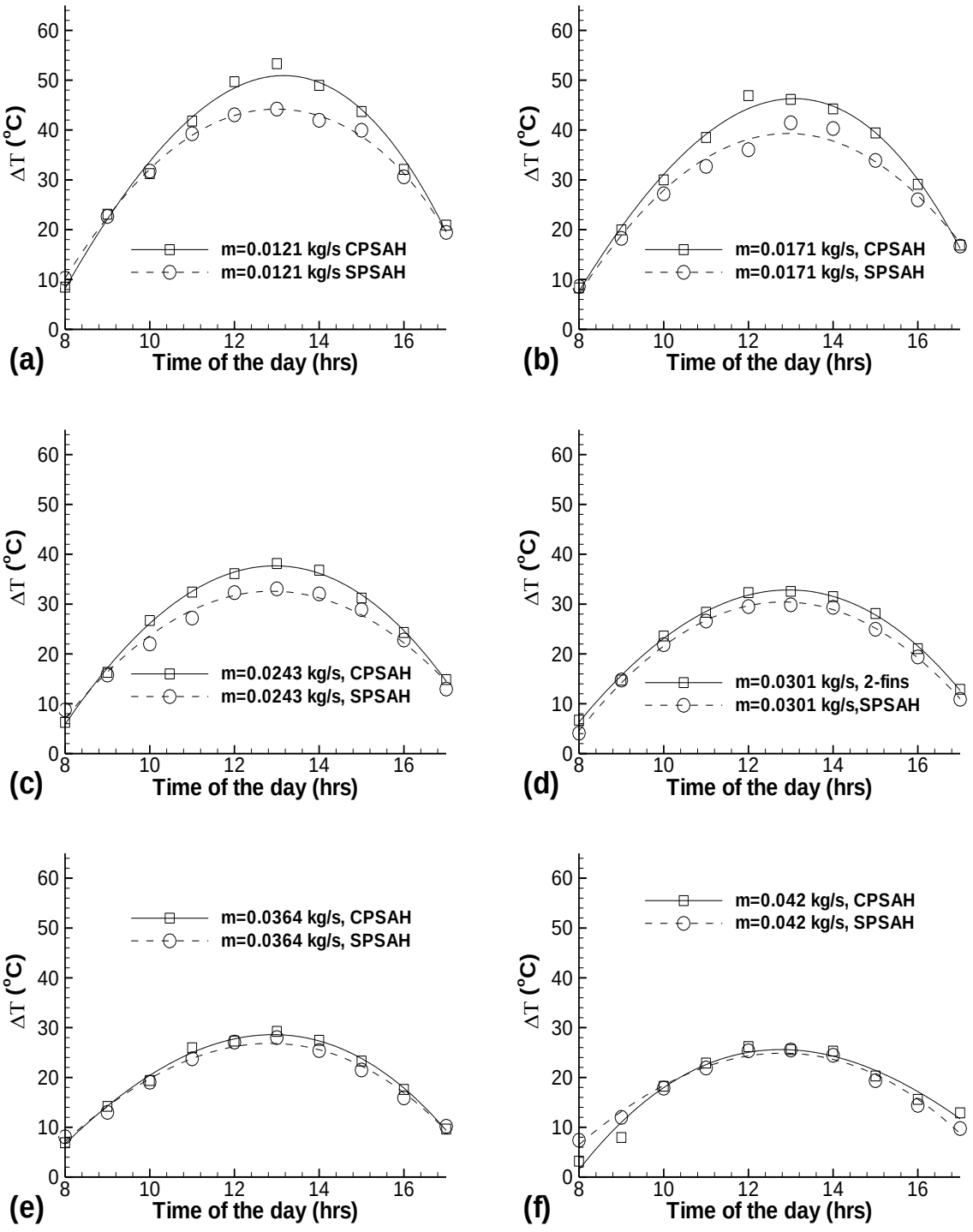

Figure 4.16: Temperature difference comparison between the 2-fins SPSAH & 2-fins CPSAH at m (kg/s) = a) 0.0121, b) 0.017, c) 0.0243, d) 0.0301 e) 0.0364 f) 0.042

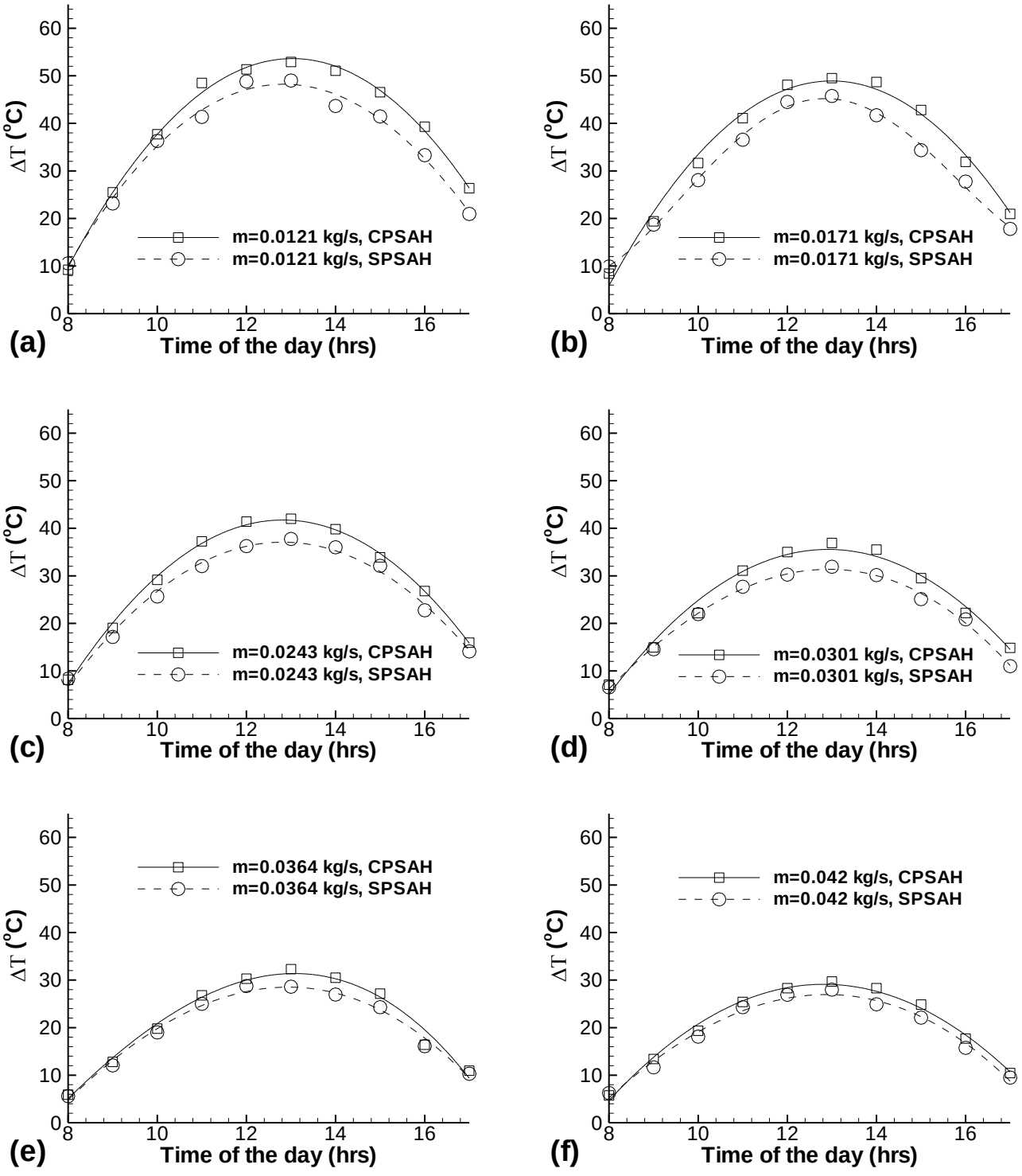

Figure 4.17: Temperature difference comparison between the 4-fins SPSAH & 4-fins CPSAH at m (kg/s) = a) 0.0121, b) 0.017, c) 0.0243, d) 0.0301 e) 0.0364 f) 0.042

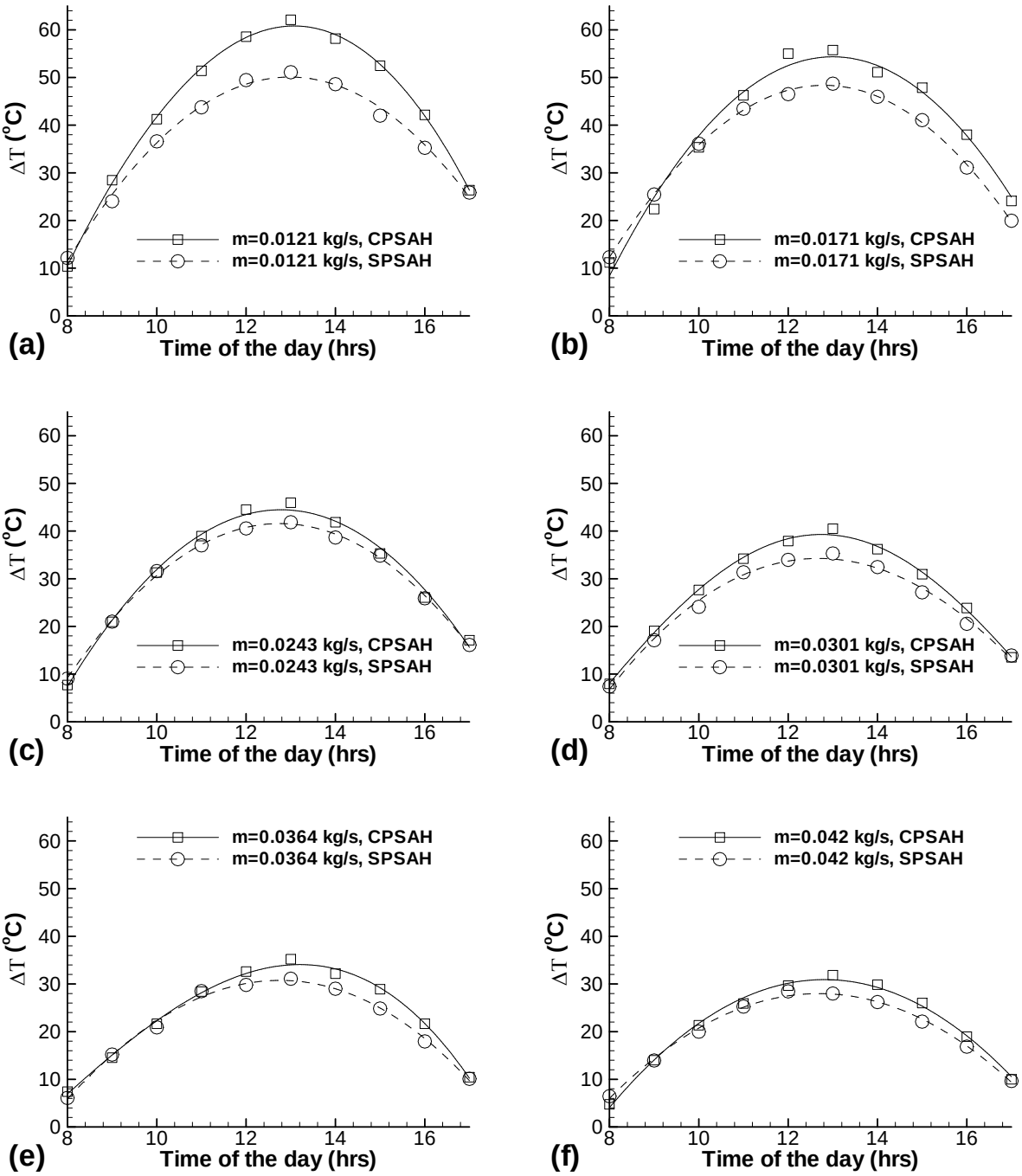

Figure: 4.18: Temperature difference comparison between the 4-fins SPSAH & 4-fins CPSAH at m (kg/s) = a) 0.0121, b) 0.017, c) 0.0243, d) 0.0301 e) 0.0364 f) 0.042

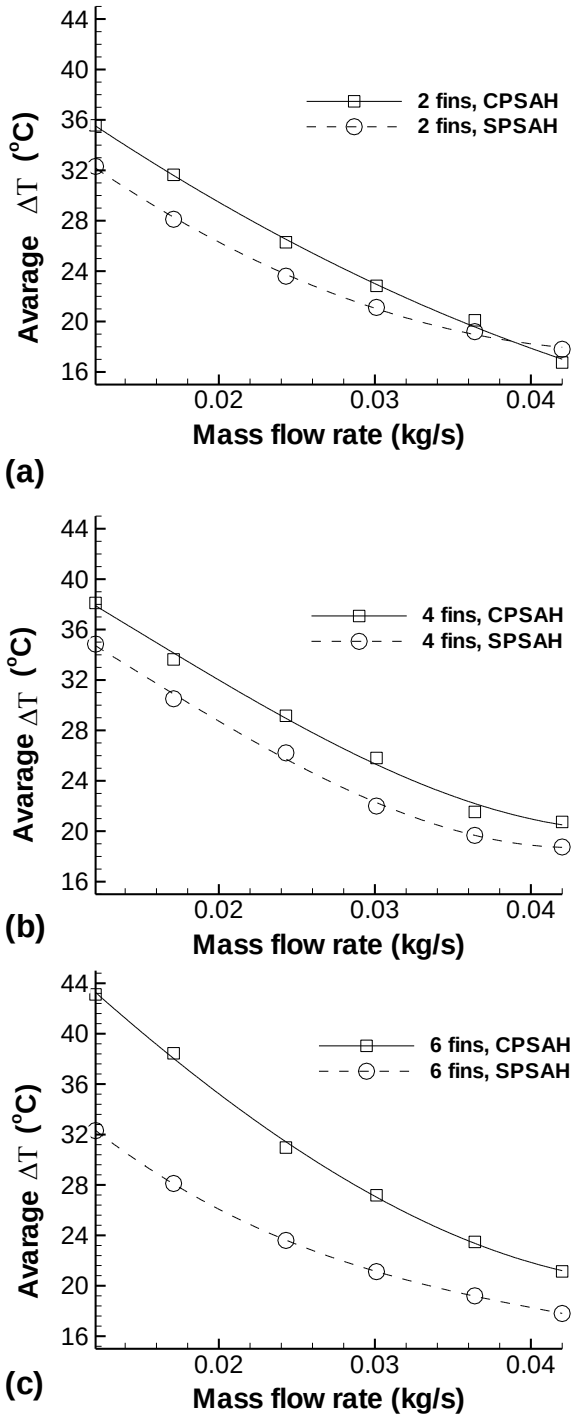

Figure 4.19: Mean average Temperature difference comparison between SPSAH and CPSAH for a) 2 fins, b) 4 fins, c) 6 fins.

4.6.2 Bed Temperature Comparison

The bed had three thermocouples equally spaced throughout the length of the wire mesh of the bed. The reading temperature of these thermocouples gives insight to potential and working fluid. A typical case, 4 fins SAH, is chosen for this study. Fig. 4.19 shows the bed temperature of SPSAH at different mass flow rates while Fig. 4.20 shows the bed temperature of CPSAH. By comparing these figures, we conclude that the bed temperature decreases as the mass flow rate increases. By increasing the mass flow rate of air, the heat transfer coefficient between the porous media and the flowing air increases. Increasing the flow rate of air means increasing the velocity acting in the porous media; thus, increasing the turbulence in the porous absorbing media. The increase of bed temperature, by decreasing the mass flow rate, increases heat losses through the glass and decreases the efficiency. The following sections will discuss the glass temperature and the efficiency of the SAH. Finally relating Figs. 4.19 and 4-20 with outlet air temperature figures in chapter 3 and chapter 4 leads to the conclusion that the outlet temperature is approximately 50-65% of the maximum temperature achieved in the wire mesh of the bed which gives an indication of the potential for an increased amount of heat to be extracted from the bed. The absorber temperature is always higher in CPSAH compared to SPSAH because the air which is based in the upper channel of the counter flow has a higher temperature than the ambient. As a result of this, the driving force of heat through the lower cover is less.

Table 4.1 : Air flow velocity (m/s) in the bed at different mass flow rate and different number of fins

m (kg/s) / Number of Fins	0.0121	0.0171	0.0243	0.0301	0.0364	0.042
2 Fins	0.2095	0.2961	0.4208	0.5212	0.6303	0.7273
4 Fins	0.4191	0.5923	0.8416	1.0424	1.2606	1.4545
6 Fins	0.6286	0.8883	1.2623	1.5636	1.8909	2.1818

Table 4.2 : ΔT_{max} at different mass flow rate and different number of fins for SPSAH and CPSAH

Max ΔT (^oC) \ m (kg/s)		0.0121	0.0171	0.0243	0.0301	0.0364	0.042
2 Fins	CPSAH	51.35	46.9	38.15	32.55	29.25	26.2
	SPSAH	44.2	44.8	33.05	29.85	28	25.7
4 Fins	CPSAH	52.9	49.5	42	36.9	32.3	29.7
	SPSAH	52	45.75	37.75	31.9	28.75	28
6 Fins	CPSAH	62.1	55.75	45.95	41.55	40.5	31.85
	SPSAH	51.1	48.7	41.85	35.3	31.1	28.45

Table 4. 3: $\Delta T_{average}$ at different mass flow rate for different number of fins

ΔT_{av} (^{o}C) \ m (kg/s)		0.0121	0.0171	0.0243	0.0301	0.0364	0.042
2 Fins	CPSAH	35.32	31.94	26.3	23.18	20.1	17.82
	SPSAH	32.31	28.12	23.58	21.12	19.2	17.8
4 Fins	CPSAH	38.84	34.25	29.345	24.92	21.29	20.32
	SPSAH	34.85	30.51	26.22	22	19.67	18.75
6 fins	CPSAH	43.12	38.7	30.96	27.57	27.15	21.23
	SPSAH	36.88	35.1	29.66	24.32	21.35	19.69

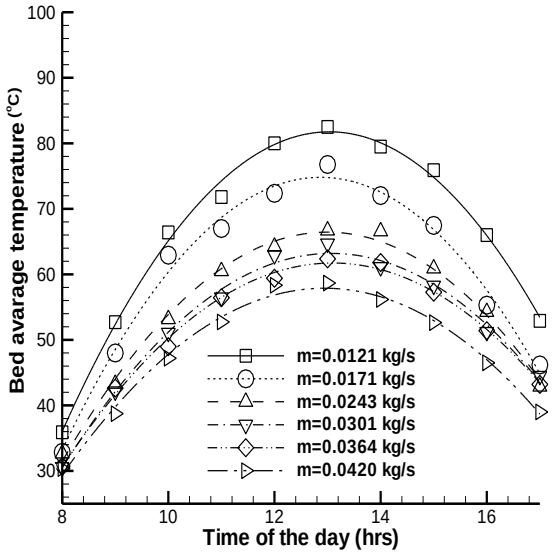

Figure 4.20: Average bed temperature at different time and mass flow rate for 4 fins SPSAH

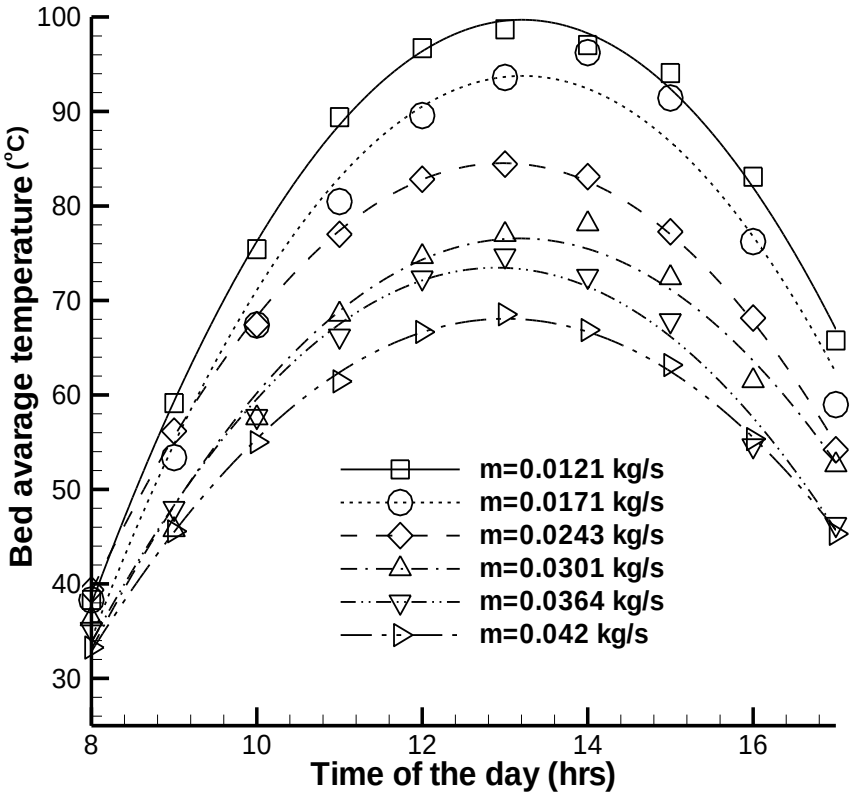

Figure 4.21: Average bed temperature at different time and mass flow rate for 4 fins CPSAH

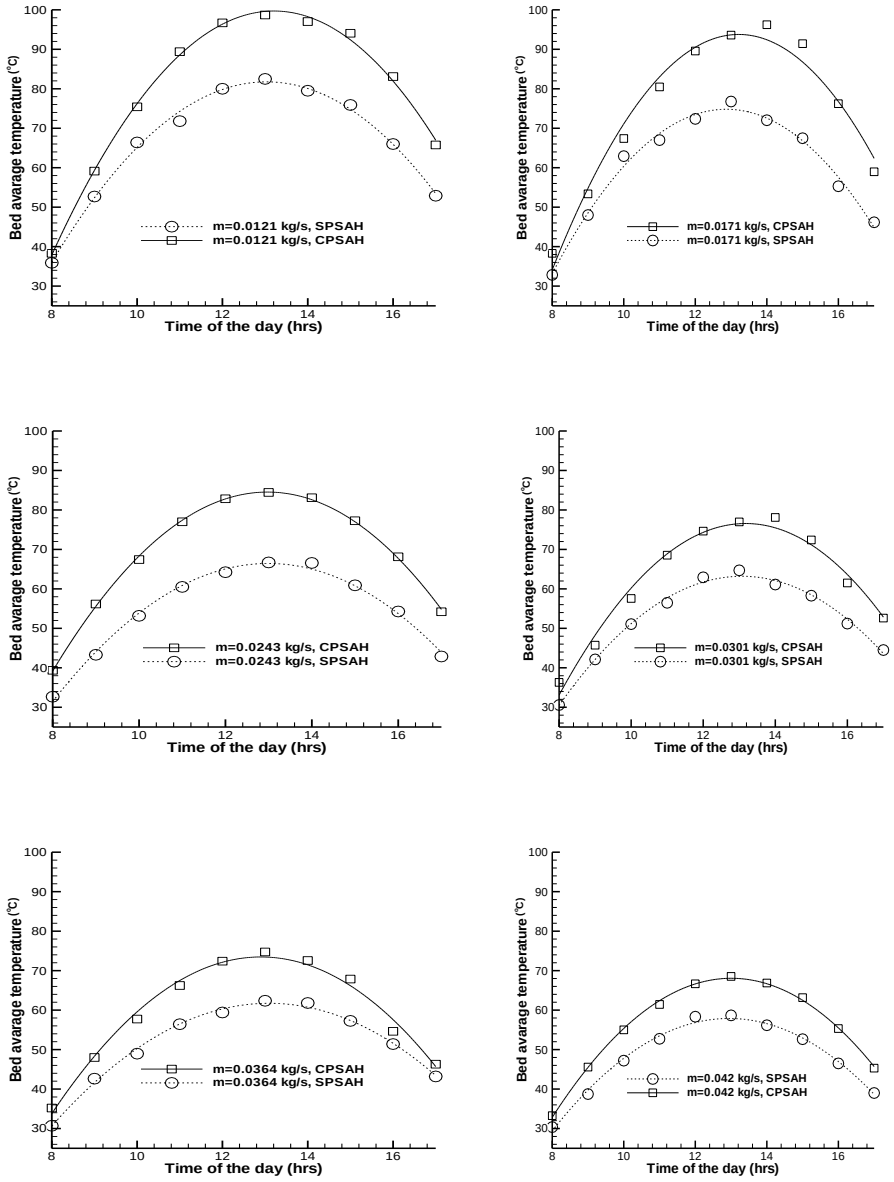

Figure 4.22: Comparison of average bed temperature at different time and mass flow rate for 4 fins CPSAH and SPSAH.

4.6.3 Glass temperature comparison

The design of the SAH affects the rate of heat transfer from the cover. Analyzing the temperature of glass is another way of studying the rate of heat lost from the cover. Figs. 4.23- 4.25 show the glass temperature difference (ΔT_g) which is defined as the difference between glass and the ambient temperature (T_g - T_{in}). In general, the glass of SPSAH is in between the upper and lower glass temperature value of CPSAH. This implies that there is more heat losses through the glazing to the surroundings from the SPSAH compared to CPSAH.

4.6.4 Efficiency Comparison

Although, in application, the important factor is the output temperature, efficiency of the SAH is important from engineering point of view. Figure 4.27 presents the comparison of glass temperature at different time and mass flow rate 2 fins CPSAH and SPSAH. The efficiency of the CPSAH is always higher than the SPSAH regardless the mass flow rate or the number of fins. Average percentage increase in efficiency of the CPSAH compared to SPSAH is not the same for all of the cases. It has been found that the percentage of increase in efficiency of the CPSAH compared to SPSAH is 17%, 21%, 19.7% for the 2 ,4, and 6 fins respectively.

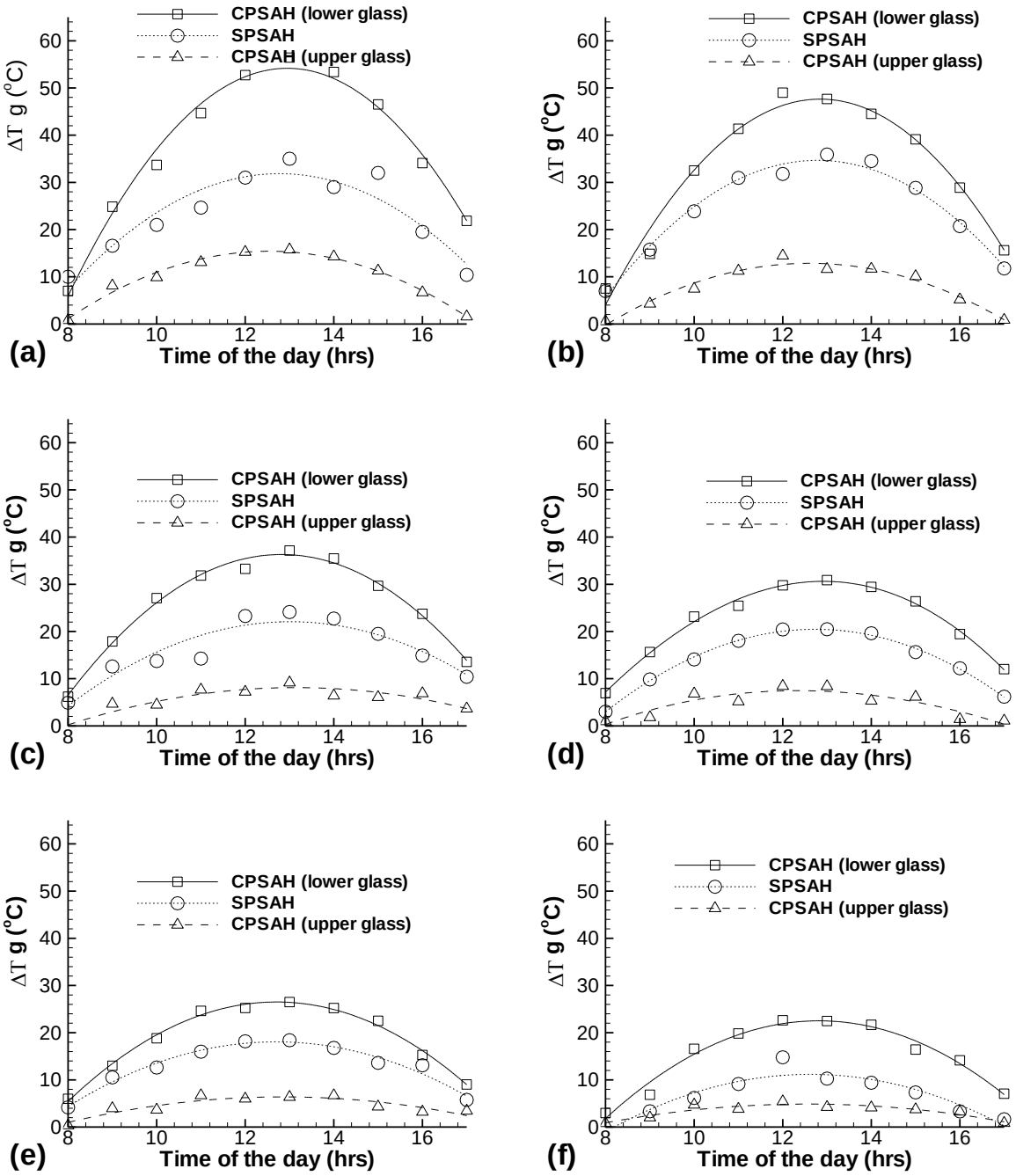

Figure 4.23: Comparison of glass temperature at different time and mass flow rate 2 fins CPSAH and SPSAH.

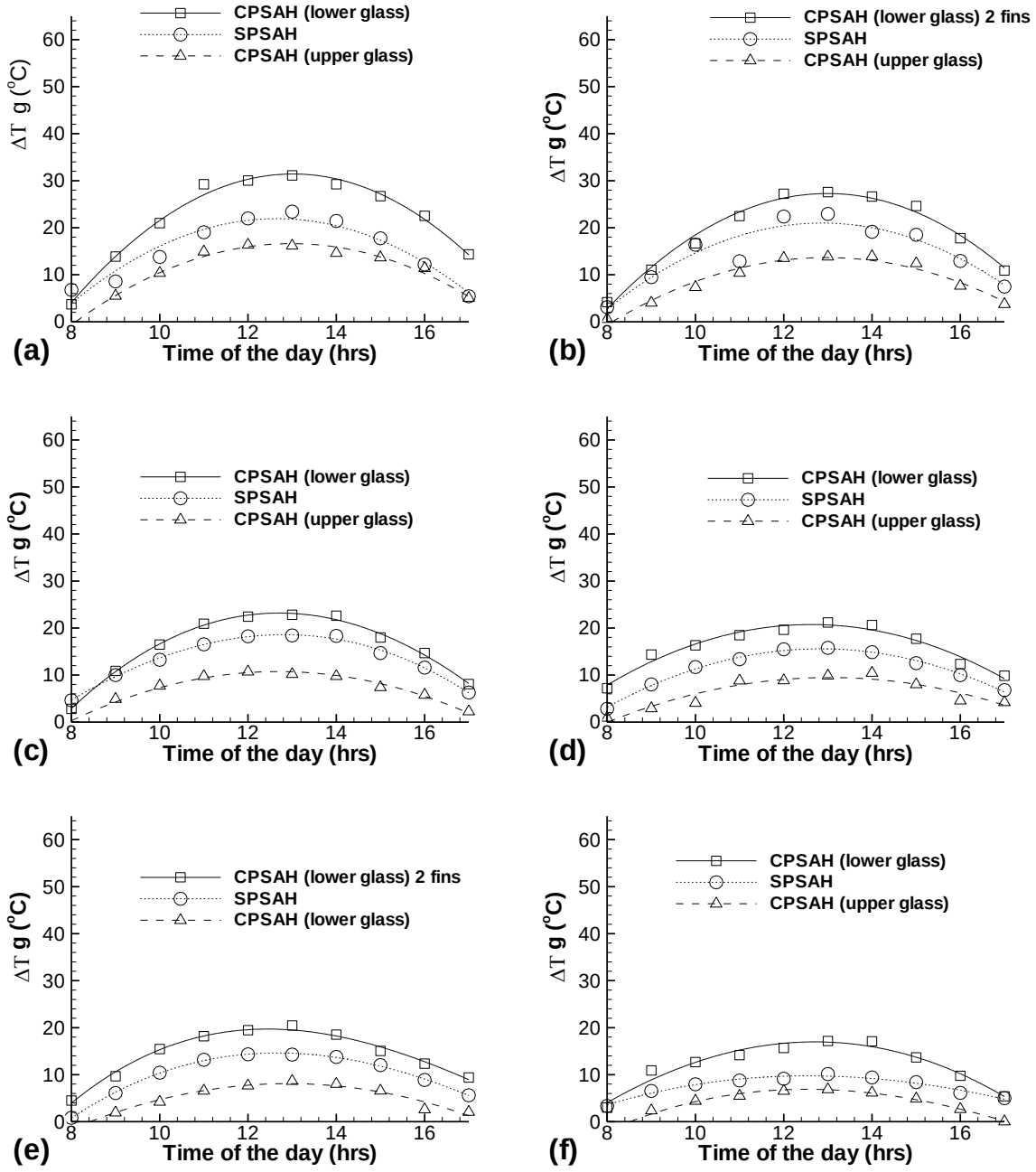

Figure 4.24: Comparison of glass temperature at different time and mass flow rate 4 fins CPSAH and SPSAH.

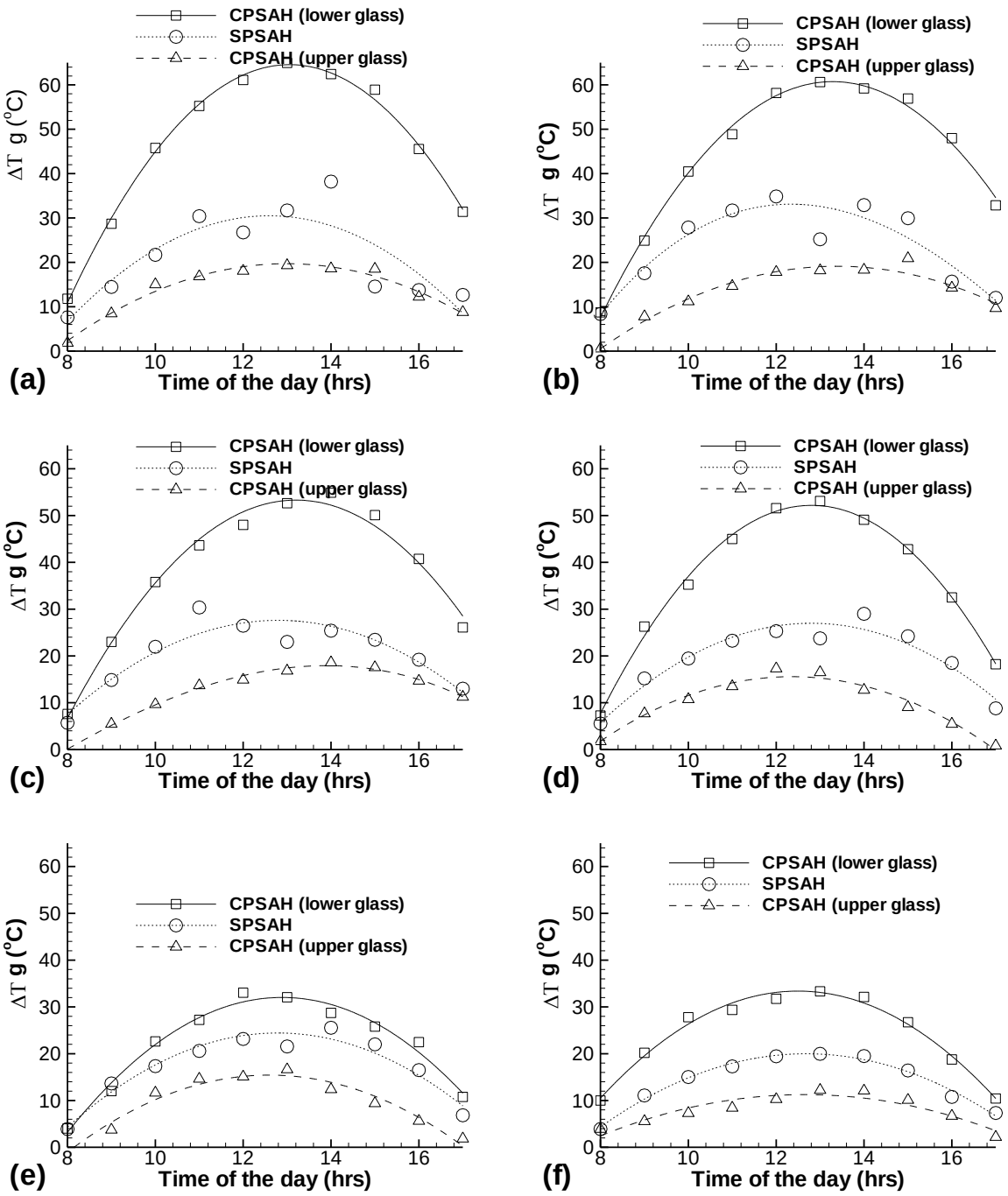

Figure 4.25: Comparison of glass temperature at different time and mass flow rate 6 fins CPSAH and SPSAH.

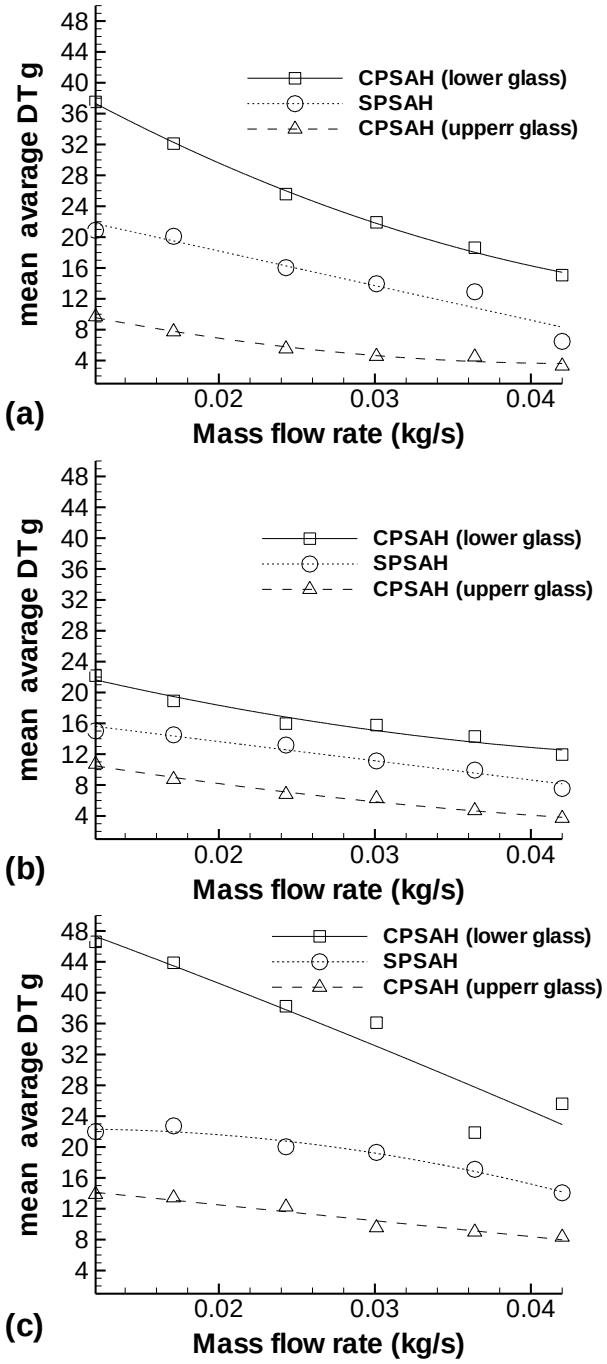

Figure 4.26: Comparison of average glass temperature of CPSAH and SPSAH at different mass flow rate for: (a)2 fins (b) 4 fins and (c) 6 fins.

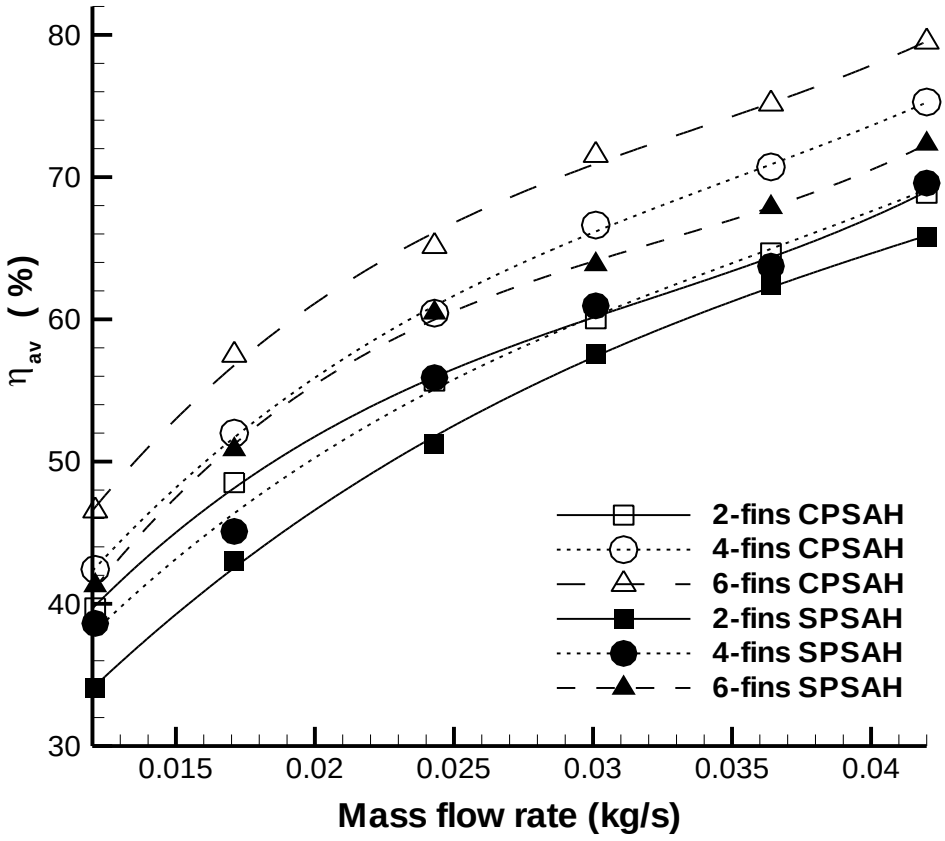

Figure 4.27: Comparison of average efficiency of CPSAH and SPSAH at different mass flow rate for: (a)2 fins (b) 4 fins and (c) 6 fins.

Chapter 5

EFFECT OF REFLECTION ON the SAHs

This chapter deals with the results of experiments that were done to investigate the effect of partitioning single flow wire mesh packed bed under Famagusta prevailing weather conditions during the summer days, 21.05.2011-05.06.2011, with a fair sky condition. In this experiment a squared shape reflector is fixed at the top of the bed tilted backward at an angle of 22^{o}. The results of the experiments are presented in this chapter. The study presented in this chapter was not conducted on the same period of the SPSAH or CPSAH. Therefore, the wind speed and relative humidity were also hourly recorded for this study. The average mean values of the wind speed and relative humidity ratio are 4.7 m/s. and 56% respectively. The technique used in measuring the flux of the sun on the SAH is not as the same as the previous experiments where the flux just was taken at the middle of the cover glass. In SPSAHWR, the glass was divided into 6 imaginary equal areas; the intensity were taken at the center of each area. The average of fluxes on these areas was considered to be the total flux on the SAH.

5.1 Reflector design and its inclination

There are different factors affecting the SAH effectiveness, such as collector dimensions, type and shape of absorber plate, glass cover, inlet temperature, wind speed and etc. There are more factors that affect the SPSAHWR, such as collector-reflector system orientation and tilt angles, collector elongation ratio, and reflector

overhanging ratio. Considering the conclusions achieved by the investigators in literature, the following achievement aims were considered:

1) The design should be practically possible, so, one meter length of reflector is found to be suitable for 1.5m length bed.
2) Overhang ratio of 10 cm was adopted to make sure that the reflected beam is concentrated at the last matrix of the bed before the exit orifice to improve the heat transfer coefficient.
3) The tilt angle of the reflector is 22^o experimentally determined at noon solar time.

The proposed geometrical design is compared with the design of others in literature. The optimized reflector angle matches with the results analytically found by Tanaka (2011) who figured that the optimum angle for latitude 30 in June is about 20^o backward from vertical.

5.2 Flux and Inlet Temperature for SPSAHWR

Figure 5.1 (a) shows the hourly variation of solar intensity versus local time of all the days during which the experiments were considered. The solar radiation was increasing from morning to a peak value at noon and then was decreasing in the afternoon until sunset. It is obvious that the increasing and decreasing is not smoothly as SPSAH and CPSAH as a result of reflection effect. The mean average values of solar radiation for the days of the experiments were $833W/m^2$, while the average concentrating factor (CF) was 1.07.

Figure 5.1 (b) shows the variation of the inlet temperature for the days the experiment conducted at different local time.

5.3 Temperature Rise through the Bed of SPSAHWR

The hourly temperature difference (ΔT) at different mass flow rates for SPSAHWR is shown in Fig. 5.2. Similar to SPSAH and CPSAH for all mass flow rates the value of ΔT increases in the morning to a peak value at noon and starts to decrease in the afternoon. The peak ΔT was achieved between 12:00 h and 13:00 h of the local time. The maximum ΔT and maximum average values ΔT obtained in the SPSAHWR were 48.1^{o}C and 35.4 ^{o}C respectively. Comparing these values with the SPSAH (having same fins number), the maximum ΔT was 44 ^{o}C and the maximum average ΔT could be reached was 32.3 ^{o}C . Table 5.1 presents the comparison of the peak and average ΔT values at different mass flow rates. The mean average increment percentage in ΔT was 18.7

5.4 Efficiency of SPSAHWR

Efficiency of the collector is an important parameter in SAHs design. Unfortunately the efficiency of SPSAHWR is always less than the SPSAH. The decrease in the efficiency is due to the excess incident heat from the reflector. Although the efficiency decreases, still fixing a reflector on the solar collector is important in some engineering applications where high temperature is needed. The average efficiency for SPSAHWR was 56.1, 51.48, 34.3, and 29.15 at mass flow rates 0.0364, 0.0301, 0.0243 and 0.0121, while the average efficiency for the SPSAH was 62.4, 57.55,51.2, 34.06 at the same mentioned mass flow rates.

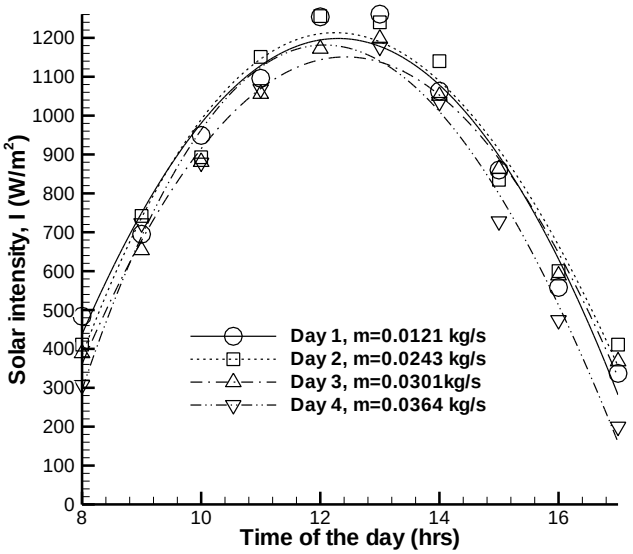

a)

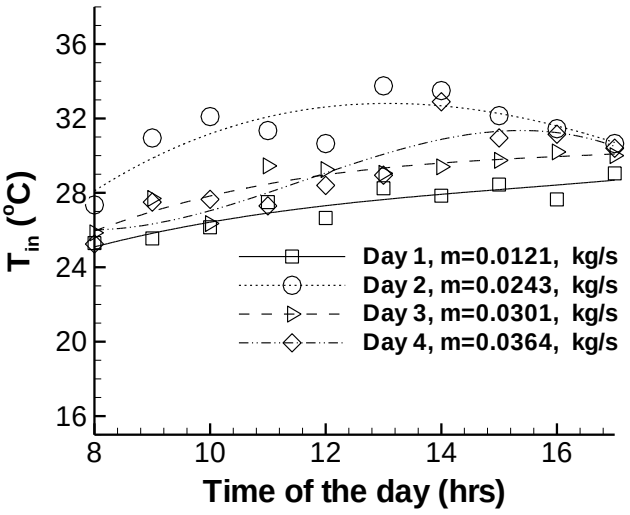

b)

Figure 5.1: a) Solar intensity b) Ambient temperatures, versus different standard local time of days for SPSAHWR

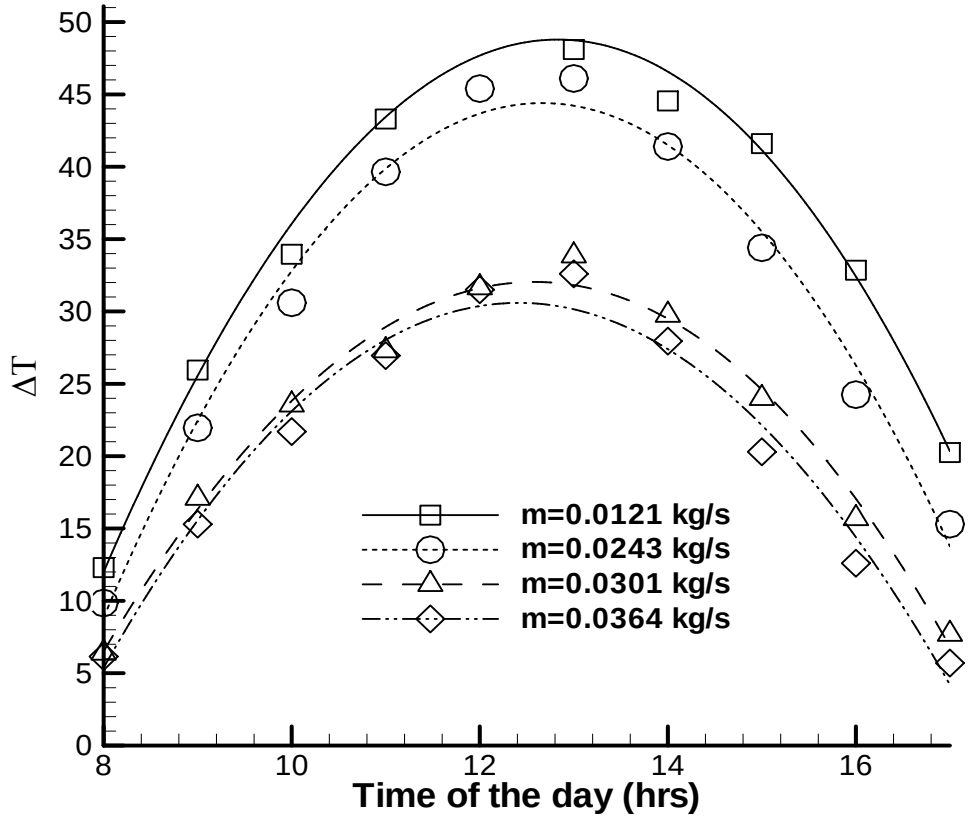

Figure 5.2: Temperature difference versus standard local time of the days at different mass flow rates for 2-fins SPSAHWR

Table 5.1: Comparison of average and peak values of ΔT between SPSAH and SPSAHWR at different mass flow rates.

Mass (kg/s)	0.0121		0.0243		0.0301		0.0364	
ΔT (^{o}C)	average	peak	average	peak	average	peak	average	peak
SPSAH	28.1	41.5	23.6	33	21.1	29.9	19.2	28
SPSAHWR	35.4	51.1	30.89	46.1	21.7	33.85	20.08	32.6

Chapter 6

CONCLUSION AND RECOMMENDATIONS

6.1 General Discussions and Conclusion

The project presents the design procedure, experimental test results and the comparison between the three different models. SPSAH and CPSAH have 2, 4 and 6 fins, while the 2 fins case is considered in the CPSAHWR to investigate the effect of reflection on the efficiency. The obtained results show that the thermal efficiency for all models increases with increasing mass flow rate of air, between 0.0121 kg/s and 0.042 kg/s. On the contrary, temperature difference between the outlet and the inlet (ΔT) was decreased with increasing mass flow rate of air. In addition, for the same air mass flow rate, the thermal efficiency increased with increasing the number of the fins. The maximum efficiency of the proposed SPSAH reached was 79.81 %, 76.19% , 71.8 % , while it was for the CPSAH 85.9 %, 82.1 % and 75.0 % at flow rate of 0.042 kg/s and for the 6, 4 and 2 fins SAHs respectively. These maximum efficiencies are obtained with lower pressure drop through the bed compared with the published data. Introducing porous media between the fins in the proposed design increased the rate of heat transfer between the flowing air and the bed. The maximum difference between the outlet and inlet air temperature for the 2, 4 and 6 fins SPSAH was 44.2 ^{o}C and 51.1 ^{o}C respectively, while the maximum difference for CPSAH was 53.3 ^{o}C 52.9 ^{o}C and 62.1 ^{o}C respectively for the same ordering of number of fins. On the other hand the maximum ΔT for the SPSAHWR was 51.5 at minimum mass flow rate

Comparing SPSAH, CPSAH, and SPSAHWR with each other leads to conclude that: The maximum temperature difference could be obtained by the 6 fins CPSAH where efficiency was also maximum.

Finally the thermal efficiency of the 6 fins SPSAH, 6 fins CPSAH, and SPSAHWR was compared with some of the reported ones. It is found that, in the proposed models; the thermal performance is enhanced compared with the other models.

6.2 Suggestions for Future Work

This study has shown the efficiency of SAHs can be improved by the use of porous material in SPSAH, CPSAH, and SPSAHWR. However there are some considerations that should be addressed for the successful design and integration of the collector into the practical life.

- Snowfall, ice, dust, debris removal for a roof top installation
- Solar powered variable speed fan is preferred to be used.
- Operate system by its actual application i.e., if it is for house heating re-circulating warm indoor air through the collector to simulate re-circulation and reheating of indoor air through the collector
- Test system with different glazing materials and not a normal window glass only
- More accurate mass flow rate measuring device can be used.

REFERENCES

Akpinar, E.K., Sarsılmaz, C., Yıldız, C., 2004. Mathematical modeling of a thin layer drying of apricots in a solar energized rotary dryer. International Journal of Energy Research 28, 739-52.

Akpinar, E.,K., Kocyigit,F. 2010. Experimental investigation of thermal performance of solar air heater having different obstacles on absorber plates. International Cominications in Heat and Mass Transfer 37, 416-421

Aboul-Enein S., El-Sebaii A.A., Ramadan M.R.I., El-Gohary H.G. 2000. Parametric study of a solar air heater with and without thermal storage for solar drying applications. Renewable Energy 21, 505-522

Aldabbagh, L.B.Y., Egelioglu, F., lkan, M., 2010. Single and double pass solar air heaters with wire mesh as packing bed. Energy 35, 3783-3787.

Alok Chaube, Sahoo, P.K.,and Solanki S.C. 2006. Analysis of heat transfer augmentation and flow characteristics due to rib roughness over absorber plate of a solar air heater. Renewable Energy 31, 317–331

Alvarez, A., Cabeza, O., Muniz, M.C., Varela, L.M., 2010. Experimental andnumerical investigation of a flat-plate solarcollector. Energy 35, 3707-3716

[a]Yeh,Ho-Ming, and Ho, Chii-Dong, 2009. Effect of external recycle on the performances of flat-plate solar air heaters with internal fins attached. Renewable Energy 34,1340–1347.

[b]Yeh, Ho-Ming, Ho, Chii-Dong, 2009. Solar air heaters with external recycle Applied Thermal Engineering 29 1694–1701.

El-Sebaii, A.A., Aboul-Enein, S., Ramadan, M. R. I., El-Bialy, E., 2007, Year round performance of double pass solar air heater with packed bed. Energy Convers Manage 48, 990-1003.

Esen, H., 2008. Experimental energy and exergy analysis of a double-flow SAH having different obstacles on absorber plates. Build Environ 43, 1046-1054.

Flores-Irigollen A. Ferna´ndez J.L., Rubio-Cerda . b, E. Poujol, F.T., 2004, Heat transfer dynamics in an inflatable-tunnel solar air heater. Renewable Energy 29, 1367–1382

Garg,H.P. and Adhikari R.S., 1999. Performance Evaluation of a single solar air heater with N-Subcollectors Connected in Different combination. Int. J. Energy Res., 23, 403-414

Goswami D.Y., Kreith F., Kreider J.F, 2000. Principles of Solar Engineering 2nd edition. Philadelphia, PA. Taylor and francis.

Gupta, M.K., Kaushik, S.C., 2009. Performance evaluation of solar air heater for various artificial roughness geometries based on energy, effective and exergy efficiencies. Renewable Energy 34, 465-476.

Hans, V. S., Saini R.P., Saini, J.S. 2009. Performance of artificially roughened solar air heaters-A review. Renewable and Sustainable Energy Reviews 13,1854-1869

Hiroshi Tanaka, 2009. Tilted wick solar still with external flat plate reflector: Optimum inclination of still and reflector. Desalination 249 411–415.

Hiroshi Tanaka, 2011. Solar thermal collector augmented by flat plate booster reflector: Optimum inclination of collector and reflector. Applied Energy 88, 1395–1404.

Ho, C.D., Yeh, H.M., Wang, R.C., 2005. Heat-transfer enhancement in double-pass flat-plate solar air heaters with recycle. Energy 30, 2796-817.

Hoa, C.D., Yeha C.W., Hsiehb, S.M., 2005, Improvement in device performance of multi-pass flat-plate solar air heaters with external recycle. Renewable Energy 30, 1601–1621.

Holman, J.P., 1989. Experimental methods for engineers. McGraw-Hill, 453 New York.

Hsieh, J.S. 1986. Solar Energy Engineering. Prentice Hall.

Hussein, H.M.S, Ahmad, G.E, Mohamad, M.A. 2000 Optimization of operational and design parameters of plane reflector-tilted flat plate solar collector systems. Energy 25, 529–542.

Kalogirou,s. 2009. Solar Energy Engineering Processes and systems. Elsevier Inc.

KOLB, A., Winter, E.R.F., Viskanta, R., 1999. Experimental studies on a solar air collector with metal matrix absorber. Solar Energy 65, 91-98.

Martin, SRL., & Fjeld, GJ. 1975. Experimental performance of three solar collectors. Energy. 17, 345-349.

Mittal, M.K., Varshney, L. 2006.Optimal thermal-hydraulic performance of a wire mesh packed bed solar air heater. Solar Energy 80, 1112-1120.

Mohamad, A.A., 1997. High efficiency solar air heater. Solar Energy 60, 71-76.

Moummi, N., Youcef-Ali, S. Moummi, A. and Desmons J.Y. 2004. Energy analysis of a solar air collector with rows of fins. Renewable Energy 29, 2053–2064.

Omojaro, A.P., and Aldabbagh, L.B.Y., 2010. Experimental performance of single and double pass solar air heater with fins and steel wire mesh as absorber. Applied Energy 87, 3759-3765.

Ozgen, F., Esen, M., Esen, H., 2009. Experimental investigation of thermal performance of a double-flow solar air heater having aluminum cans. Renewable Energy 34, 2391-2398.

Paisarn, N., 2005. Effect of porous media on the performance of the double-pass flat plate solar air heater. Int Comm Heat Mass Transf 32, 140–150.

Prasad,S.B., Saini, J. S., Singh Krishna, M., 2009. Investigation of heat transfer and friction characteristics of packed bed solar air heater using wire mesh as packing material. Solar Energy 83, 773-783.

Romdhane, ben salma, 2007.The air solar collectors: Comparative study, Introduction of baffles to favor the heat transfer. Solar Energy, 139-149.

Shanmugam, V. and Natarajan, E. 2007. Experimental study of regenerative desiccant integrated solar dryer with and without reflective mirror. Applied Thermal Engineering 27,1543–1551.

Sopian, Supranto, M.Y. Othman, W.R.W. Daud, B.Yatim. 2007, Double-pass solar collectors with porous media sutable for higher-temperature solar- Assisted Drying systems; Jurnal of energy Engineering 13, 9402 133 -1 13.

Suleyman Karsli, 2006. Performance analysis of new-design solar air collectors for drying applications. Renewable Energy 32 , 1645–1660.

Tchinda, Rene,2009, A review of mathematical models for predicting solar air heaters systems. Renewable and Sustainable Energy Reviews 13,1734-1759

Thakura, N.S., Sainib J.S. , Solankib S.C. 2003, Heat transfer and friction factor correlations for packed bed solar air heater for a low porosity system, Solar Energy 74 319–329.

Tyagi, S.K., Shengwei Wang , M.K. Singhal, Kaushik S.C, Parkd, S.R. 2007. Exergy analysis and parametric study of concentrating type solar collectors. International Journal of Thermal Sciences. 46, 1304–1310.

Varuna , Sainib, R.P., Singalb, S.K. 2008, Investigation of thermal performance of solar air heater having roughness elements as a combination of inclined and transverse ribs on the absorber plate. 33, 1398–1405

Varun, Amar, Patniak,R.P.Saini, S.K.,Signal, Siddhartha, 2009. Performance prediction of SAH having roughened duct provided with transverse and inclined ribs as artificial roughness. Renewable Energy 34, 2914-2922.

Yeh,H.M.,Ho,C.D. 2009. Solar air heaters with external recycle. Applied Thermal Engineering 29, 1694-1701

Youcef-Ali, S., 2005. Study and optimization of the thermal performances of the offset rectangular plate fin absorber plates, with various glazing. Renewable Energy 31, 271-280.

Youcef-Ali,S, and Desmons, J.Y. 2006. Numerical and experimental study of a solar equipped with offset rectangular plate fin absorber plate. Renewable Energy 31, 2063–2075.

Youcef-Ali, S., and Desmons J.Y. 2007. Influence of the aerothermic parameters and the product quantity on the production capacity of an indirect solar dryer 32, 496–511.